CYCLE SYMMETRY AND ITS CAUSES, CISCO GROUP (VIRGILIAN AND WOLFCAMPIAN), TEXAS

WAN YANG*
Department of Geological Sciences, The University of Texas at Austin, Austin, Texas 78712, U.S.A.

ABSTRACT: **181 transgressive–regressive cycles composed of nonmarine and marine carbonate and siliciclastic rocks of the Cisco Group on the Eastern Shelf, Texas, display complex characteristics at both hemicycle and full-cycle scales. They are delineated on the basis of successive changes of depositional environments, stratal boundary relations, and stratigraphic position. Transgressive and regressive stratigraphic environment gradients are defined as the magnitude of environmental shift divided by thickness for each hemicycle. They indicate the rates of lateral environmental shifts during transgression and regression. Cycle symmetry index is defined as the ratio between transgressive and regressive stratigraphic environment gradients. It provides a measure of stratigraphic response to controlling processes.**

Most Cisco cycles are asymmetrical with steep transgressive and shallow regressive stratigraphic environment gradients, indicating cyclic but asymmetrical variations of major allogenic processes over a cycle interval. These systematic variations are delineated from climate-sensitive rock types, stratal thickness, and sedimentary features. The relative dominance of processes controlling accommodation (i.e., glacio-eustasy and basement subsidence) versus those controlling sedimentation (i.e., climate, upland sediment yield, and sediment supply at the depositional site) determines cycle symmetry. A formulated relation between cycle symmetry index (i.e., stratigraphic response) and rates of these processes demonstrates that transgressive sedimentation is controlled by sediment supply, whereas regressive sedimentation is controlled by accommodation. This relation is potentially useful in quantitatively predicting stratigraphic responses to specific allogenic processes in cyclic sedimentation.

Five Cisco cycle types defined by the type of component lithofacies display the stratigraphic response mainly to noncyclic allogenic and autogenic processes. The cycle types have varying magnitude, thickness, and symmetry. They also vary in lateral extent and in abundance. A process-response model of cyclic sedimentation of the Cisco Group on the Eastern Shelf is established. It emphasizes the interplay between autogenic and allogenic processes at the sub-cycle scale. Understanding interactions among glacio-eustasy, climate, shelf subsidence, sediment supply, and depositional dynamics during various stages of transgression and regression is central to a clearer comprehension of the observed variations in cycle characteristics.

INTRODUCTION

Meter-scale depositional cycles are the building blocks of larger-order stratigraphic units, such as depositional sequences (e.g., Barrell 1917; Goldhammer et al. 1994). Systematic spatial and temporal stacking of cycles or parasequences has enabled geologists to establish a basinwide stratigraphic framework and to speculate on the processes controlling cycle formation (e.g., Wilson 1967; Posamentier et al. 1988; Brown et al. 1990). Each cycle is a stratigraphic entity. A close examination of these cycles at sub-cycle and full-cycle scales will enable us to better understand the roles and mechanisms of various processes and their stratigraphic responses (e.g., Wanless and Shepard 1936; Soreghan 1994).

Tectonics, glacio-eustasy, climate, and depositional dynamics have been invoked as major controls for late Paleozoic transgressive–regressive cycles and depositional sequences (e.g., Wanless and Shepard 1936; Brown 1969; Brown et al. 1990; Heckel 1977, 1986; Ross and Ross 1985; Klein and Willard 1989; Cecil 1990). Any single process/control cannot explain the complex cycle characteristics (e.g., Galloway and Brown 1972; Heckel 1984; Yancey 1991). Regional cycle correlation has been effective in delineating regional trends and the major controls (mainly eustatic sea-level changes) of cyclic sedimentation (e.g., Boardman and Heckel 1989; Connolly and Stanton 1992), but yields only a limited level of understanding of the processes and mechanisms in cyclic sedimentation (Laporte and Imbrie 1964).

This study emphasizes the need to integrate contemporaneous autogenic and allogenic processes in order to understand the interplay among these processes as well as corresponding stratigraphic responses during both transgression and regression. Integration is achieved quantitatively by defining stratigraphic response as cycle symmetry and formulating the relation between cycle symmetry and major allogenic processes via a one-dimensional model of cyclic sedimentation in a shallow shelf setting. The control of a specific process on cycle symmetry can be investigated via this relation. This approach lays a foundation for quantifying stratigraphic responses and major allogenic controls on cycle formation and cycle architecture.

The quantitative approach is applied to transgressive–regressive cycles of the Upper Pennsylvanian and Lower Permian Cisco Group, Eastern Shelf, north-central Texas. The symmetry of the Cisco cycles can be explained by the systematic variations of major controlling processes. A shallow shelf process–response model is established to illustrate the interaction between allogenic and autogenic processes during deposition of the Cisco cycles. Process-oriented stratigraphic analysis at the sub-cycle scale elucidates the roles of these processes in intra-cycle and inter-cycle variations of cycle characteristics (Swift and Thorne 1991). It will facilitate regional cycle correlation, and is essential to interpreting sequence-scale stratigraphic development (Goldhammer et al. 1994).

Transgressive–regressive cycles of the Cisco Group were deposited on the Eastern Shelf, which was located in the equatorial wet belt and isolated from the other North American basins by tectonic uplifts (Figs. 1–4; Brown et al. 1990; Witzke 1990). 88 measured sections are distributed in the outcrop belt of $\sim 200 \times 40$ km^2 (Fig. 1), and 181 distinct cycles are delineated (Yang 1995). Cycle attributes are used to define stratigraphic response, to clarify the roles of various processes in cycle formation, and to establish the foundation for a process-response model of cyclic sedimentation.

ATTRIBUTES OF TRANSGRESSIVE–REGRESSIVE CYCLES

The Cisco cycles are defined by their attributes—magnitude, thickness or duration, and symmetry. The depositional environment of each rock unit is interpreted prior to cycle analysis from outcrop and petrographic data on the basis of lithology, fossil assemblage, sedimentary structures and textures, and lateral and vertical relationships with adjacent facies (Table 1; Yang 1995). Upward-deepening and -shallowing trends of depositional environments are interpreted from successive changes of depositional environments, stratal boundary relations, and stratigraphic position. They indicate repeated landward and seaward shoreline movement, i.e., transgression and regression. Each pair of upward-deepening and -shallowing trends defines a transgressive–regressive cycle (Fig. 5; Wanless and Shepard 1936).

The magnitude of transgressive or regressive intervals or hemicycles is defined as the change of depositional environments over the transgressive

* Present address: Phillips Petroleum Co., 1440E Plaza Office Building, Bartlesville, Oklahoma 74004, U.S.A.

JOURNAL OF SEDIMENTARY RESEARCH, VOL. 66, NO. 6, NOVEMBER, 1996, P. 1102–1121
 1073-130X/96/066-1102/$03.00

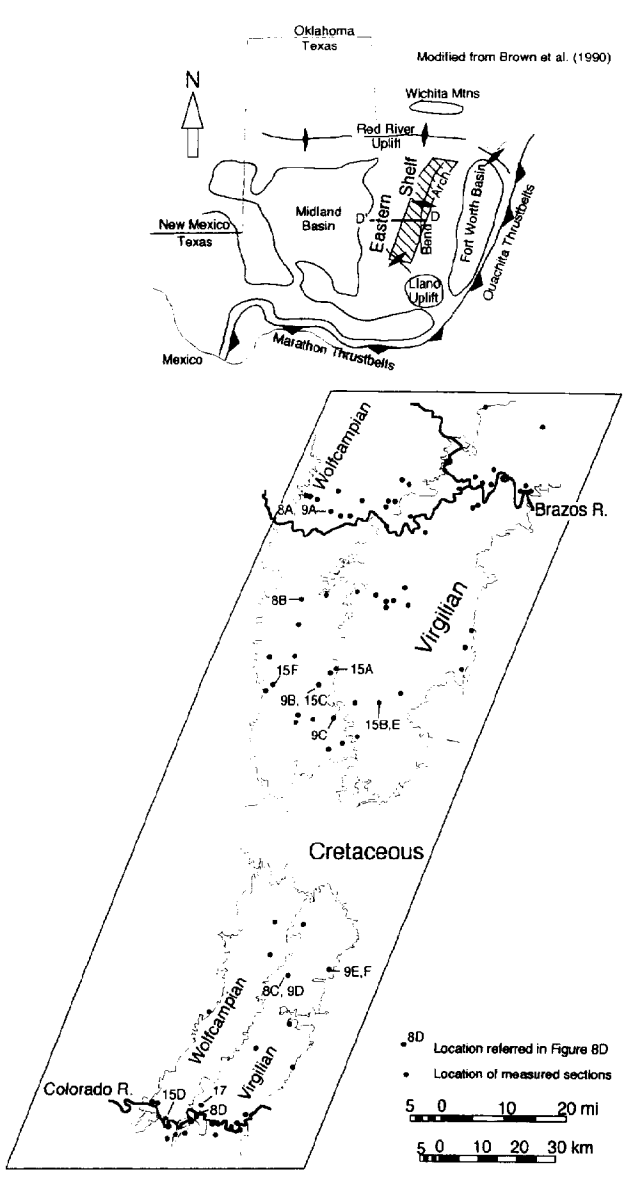

FIG. 1.—Tectonic map of north-central Texas and simplified geologic map of the Cisco Group in the outcrop as well as locations of measured sections in this study. The location of the cross section in Figure 3 is also shown.

or regressive intervals, which indicates the extent of transgression or regression (Figs. 5, 6A, B). Cycle magnitude is taken to be the larger of the transgressive and regressive magnitude. The magnitude may also be defined using objective measurements of rock properties, such as isotope ratio and carbonate content for cycles composed of simple lithologies. Cycle duration can be inferred from cycle thickness and magnitude. Assuming a constant sedimentation rate for all sediments, or steady transgression and regression, thicker or higher-magnitude cycles should have longer duration. Although both assumptions are incorrect, to a first approximation a thick and high-

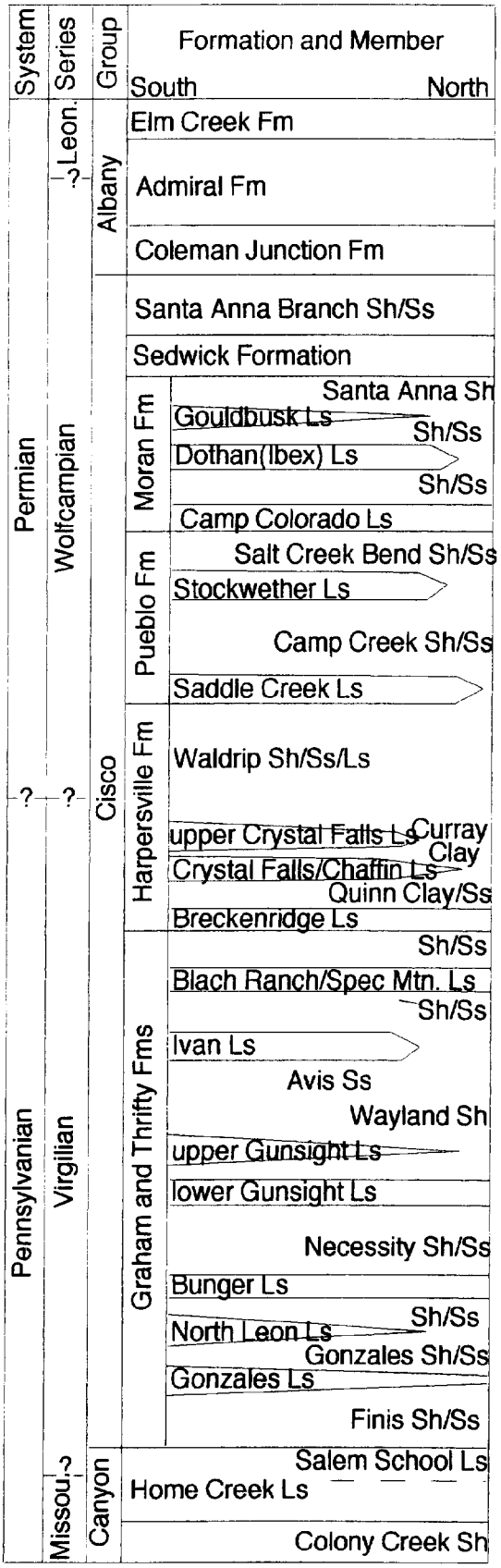

FIG. 2.—Formal outcrop formations and members, Virgilian and Wolfcampian Series, Eastern Shelf, north-central Texas. No vertical scale intended. Modified from Brown et al. (1990). Leon., Leonardian; Missou., Missourian.

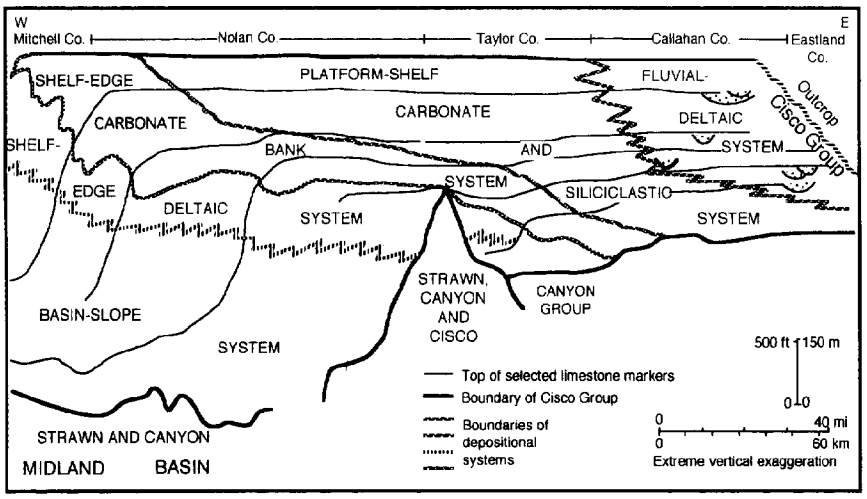

FIG. 3.—Dip stratigraphic cross section of the Cisco Group showing the progradational and aggradational configurations of the Eastern Shelf and depositional systems of the Cisco Group. Location of the section is shown in Figure 1. Horizontal scale is approximate. Highly simplified from Section D–D′ of Brown et al. (1990).

magnitude cycle probably spans a longer time interval than a thin and low-magnitude cycle.

Cycle symmetry measures the differences between transgressive and regressive hemicycles in: (1) magnitude of environmental shift, (2) stratigraphic thickness, and (3) number and type of component lithofacies. Magnitude and thickness can be combined to define the transgressive or regressive stratigraphic environment gradient (abbreviated as stratigraphic gradients in this paper) as the magnitude of environmental shift divided by the thickness of respective hemicycles. Cycle symmetry is defined as the ratio between regressive and transgressive stratigraphic gradients, termed here cycle symmetry index (SI) (Fig. 6C).

A stratigraphic gradient is the rate of environmental shift in stratigraphic space. It can be used to estimate the rate of shoreline transgression or regression if cycle duration (or sedimentation rate) is known. Assuming that thickness is proportional to time, cycle SI is the ratio between the average rates of environmental shifts during transgression and regression. A symmetrical cycle has an SI value equal to one, indicating an equal pace of environmental shift during transgression and regression. An asymmetrical cycle has an SI value larger or smaller than one (Fig. 6D).

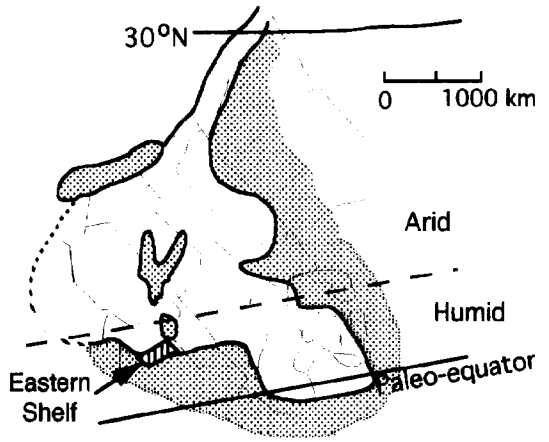

FIG. 4.—Interpreted paleogeography of the western United States for the Late Carboniferous (Missourian and Virgilian). Continental margins and distribution of land areas (lightly shaded area) during maximum marine onlap are schematic. Eastern Shelf (heavily shaded area) is approximately located in the northern humid zone north of the paleo-Equator. Simplified from Witzke (1990).

Cycle symmetry index is a quantitative measure of stratigraphic response combining both magnitude and thickness. It is determined by processes controlling the thickness and magnitude of transgressive and regressive intervals and thus provides a tool to quantitatively assess the roles of various processes in cycle formation at the sub-cycle scale. Systematic changes of cycle SI along depositional dip and strike may indicate the changing roles of various controlling processes, and cycle SI can be used for cycle classification in various geologic settings. The potential of this index awaits future exploration.

SIs are calculated for 162 complete or nearly complete Cisco cycles by ranking depositional environments (Fig. 6B). Ranking is necessary in this study because paleo–water depths of many sedimentary facies, especially the maximum-transgressive core shale, fluvial deposits, and paleosols, could not be confidently estimated. This problem can be eliminated if objective measurements are used to define cycle magnitude. Cycle symmetry is not affected by not using absolute paleo–water depth estimates, but SI values, except SI = 1, are affected because of nonuniform calibration of paleo–water depth to environment ranks (Fig. 6B, C). The majority of Cisco cycles have SIs smaller than one and thus are asymmetrical with a faster transgressive environmental shift (steeper stratigraphic gradient) and a slower regressive shift (shallower stratigraphic gradient) (Fig. 7A).

Cycle symmetry index, however, ignores the differences in the number and type of component lithofacies between transgressive and regressive hemicycles. These differences are reflected in the types of Cisco cycles (Table 2, Fig. 8): Type I is the typical midcontinent "Kansas-type" cyclothem (Fig. 9A; Heckel 1977); Type II has a coalesced transgressive and regressive limestone and no maximum-transgressive core shale (Fig. 9B); Type III is similar to the typical "Illinois-type" cyclothem, without transgressive limestone (Wanless and Shepard 1936); Type IV does not have regressive limestone; and Type V is composed entirely of siliciclastics. Types III, IV, and V may or may not contain core shales. Cycle classification based on the number and type of defining component lithofacies is practical in the field. It emphasizes the varying roles of sedimentary processes at different stages of cycle formation. Types II and I cycles are the most abundant (Fig. 10A).

Cycle types display the aspect of stratigraphic response to processes controlling lithofacies development. In regard to component lithofacies, Types I, II, and V cycles are lithologically symmetrical, having similar number and type of major component lithofacies between the hemicycles (Table 2). Comparison of cycle SI distribution of different cycle types indicates that the majority of the lithologically symmetrical cycles of Types I, II, and V have SIs smaller than one, as do the lithologically asymmetrical

TABLE 1.—*Sedimentary characteristics and depositional environments of transgressive-regressive cycles of the Cisco Group.*

Stages		Component lithology	Fossil assemblage	Sedimentary structures and textures	Boundary relations	Depositional environments	Thickenss
Regression	Maximum	Paleosol (> 80%). Ss & conglomerate; variegated, red, or purple. 30% multistory; vertisol or inceptisol; minor sh in mud plugs	Rare to none	Root mold; calcic/clay nodule horizon; slickenside; soil ped; clay cutan. Coarse to medium, trough & planar x-beds; channel geometry	Diffusive or gradational. Erosional; relief < 10 m	Semi-arid with a pronounced dry season, sparsely wooded grassland (Retallack, 1990); developed mostly on parent fluvial and deltaic sediments. Fluvial, incised valley	10 cm–~20 m; 85% 1–15 m; 60% < 4 m. < 10 m
	Late	SS & sh; sandy, rarely carbonaceous; ss hematitic; conglomerate at base	Rare plant remains	Large-medium trough & planar x-beddings	Sharp, erosion, or gradational, frequent facies changes	Shoreline, delta plain, fluvial	> 1–2 m; commonly > 5 m; ss > 1–2 m
		Sh & ss, sand-rich, commonly ferruginous; local thick deltaic ss	Rare; local low-diversity marine fossils; some plant remains	Current-flow structures. Mostly noncalcareous	Sharp or gradational	Mudflat, tidal channel, beach, delta, prodelta	> 80–90 cm
	Early	Grainstone & packstone, arenaceous & ferruginous, some algal bioherms; some as soils; capped by thin ferruginous claystone, ironstone, or *Myalina* coquina	Low-diversity fauna	Cryptalgal lamination; boring; fenestrae; abraded & altered, coated/encrusted grains; *Osagia*	Sharp or gradational	Restricted to semi-restricted, episodically exposed tidal flat	< 10 cm–> 10 m; most 20–50 cm, 60–80 cm, 1–4 m
		Packstone & minor wackestone	Very fossiliferous	Highly burrowed		Lower intertidal to shallow subtidal; some fairly deep	
		Packstone & wackestone	Mixed fauna	Highly burrowed			
Transgression	Maximum	Dark gray sh; some silty or phosphatic; 30% are calcareous with rare ls nodule, few thin, arenaceous & argillaceous wackestone tempestites	Disseminated plants in some cycles; sparse-fairly abundant megafossils; micro-fossils not studied. Mixed fauna in turbidites	Well-laminated to massive, blocky Turbidites graded, well current-laminated	Sharp	80% deeper than fair-weather wavebase; very shallow to shallow in Types III, IV, and V cycles; most hemipelagic & prodeltaic	< 10 cm–> 10 m; most 40–70 cm & 1–4 m
	Late	Argillaceous/arenaceous wackestone & mudstone. Skeletal packstone & wackestone. Packstone, grainstone, arenaceous, common extraclasts; conglomerate lags	Thin brachiopod, crinoid, fusulinid, mm gastropod, spicule, trolibote, phylloidal algae, ostracod, bryozoan	Lower part common current-laminated. Upper part bioturbated or massive. Well-bedded, medium-thick	Gradational or sharp; occasionally sharp or erosional contacts with underlying cycle	70% lower intertidal to subtidal; some fairly deep subtidal; few below fair-weather wavebase; normal, open, low-high energy. Upward deepening.	< 0.1–10 m; most 20–50 cm & 1–2 m
	Early	Sh dominant, commonly calcareous; some sandy; some with upward-increasing ls nodule. Ss commonly calcareous, some conglomerates	30% sh fairly fossiliferous; thin-walled brachiopod, crinoid, bryozoan, mm-size gastropod, fusulinid, pelecypod; some plant-rich. Fossils or molds in ss.	Burrowed to highly burrowed; ripple marks and herring-bone x-bedding fairly common	Gradational. Or sharp/erosional with underlying cycle	Mudflat, tidal channel, barrier, bar, back-barrier	< 0.1 to > 5 m; most 20–50 cm in Types I, II, IV cycles; 1–3 m in Types V, III cycles
		Interbedded ss & sh; sheet ss; basal carboniferous sh & lignite	Plant remains, freshwater molluscs	Bioturbation; current-flow structures	Sharp to erosional; occasionally gradational	Delta plain, estuarine, strandplain	Usually < 2 m

cycles of Type IV (Fig. 7). Approximately one-half of the lithologically asymmetrical Type III cycles have SIs smaller than one, the other half have SIs larger than one. More than 40% of Types II and IV cycles have SIs less than 0.2. There is no demonstrable relation between cycle SI and cycle type, suggesting that different processes, or different mechanisms of the same processes, separately control lithofacies and stratigraphic gradient, as discussed later in this paper.

CYCLE SYMMETRY AND ITS CONTROLLING PROCESSES

Nature of Cycle Symmetry Index

Cycle SI is an indicator of the symmetrical or asymmetrical variations of processes that control the magnitude and thickness of transgressive and regressive hemicycles. The relation between cycle symmetry and major processes is established via a one-dimensional model involving creation and infilling of accommodation space in a shallow-shelf setting, such as the Eastern Shelf (Fig. 11). This model assumes asymmetrical base-level changes, and nonconstant basement subsidence and sedimentation during transgression and regression. Accommodation space is defined as the distance between base level and the top of the underlying cycle, whereas depositional space is the distance between base level and sediment surface (Fig. 11; see also Posamentier et al. 1988, Bond and Kominz 1991). The depositional space is equivalent to paleo–water depth for subaqueous environments. Base level could be any equilibrium surface, such as the absolute sea level or a graded river profile (Barrell 1917; Wheeler 1964). The former caps the submarine accommodation space, the latter caps the subaerial accommodation space. The variables in this model may vary so as to simulate specific scenarios of marine and nonmarine sedimentation. For example, the case in which the amplitude of sea-level rise (C_1) is larger than that of sea-level fall (C_2) simulates superimposition of high-frequency sea-level cycles on the rising limb of a low-frequency sea-level cycle; the case of $C_1 < C_2$ simulates superimposition on the falling limb; and the case of $C_1 = C_2$ simulates a low-frequency sea-level stillstand (Fig. 11).

A fundamental assumption is implied in the simple model: the absolute

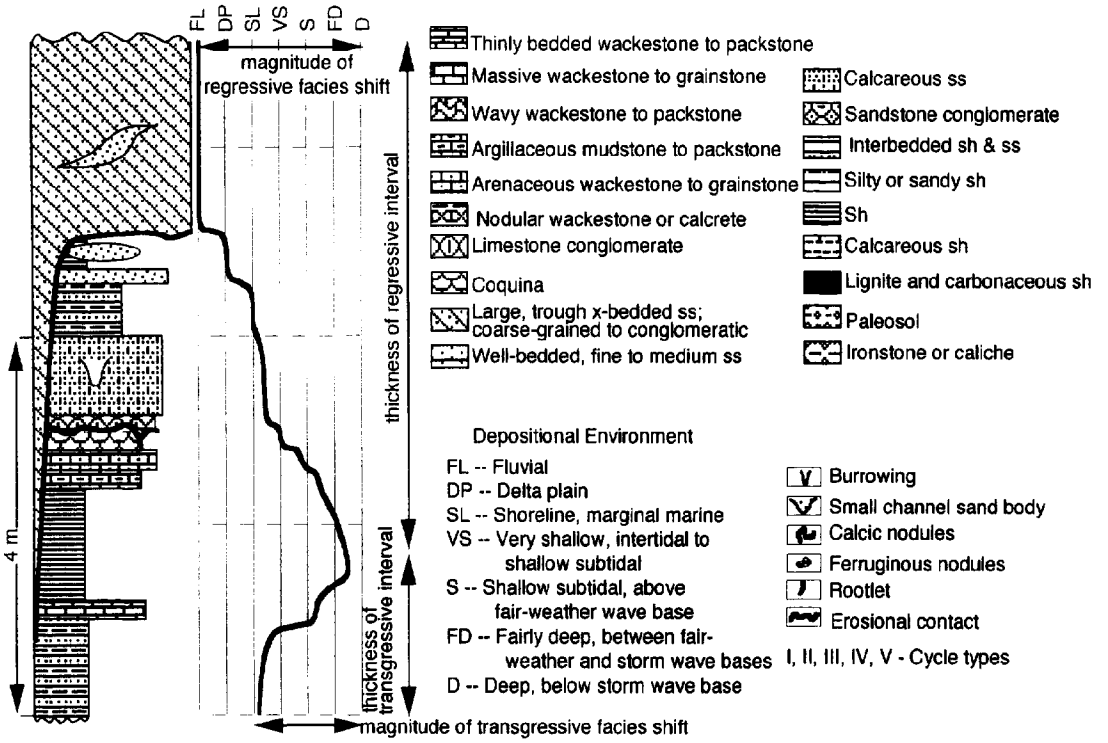

FIG. 5.—Diagram showing a measured section (left panel) and environmental interpretation of each lithofacies as the thick curve on a grid (right panel). Cycle magnitude and thickness are also defined.

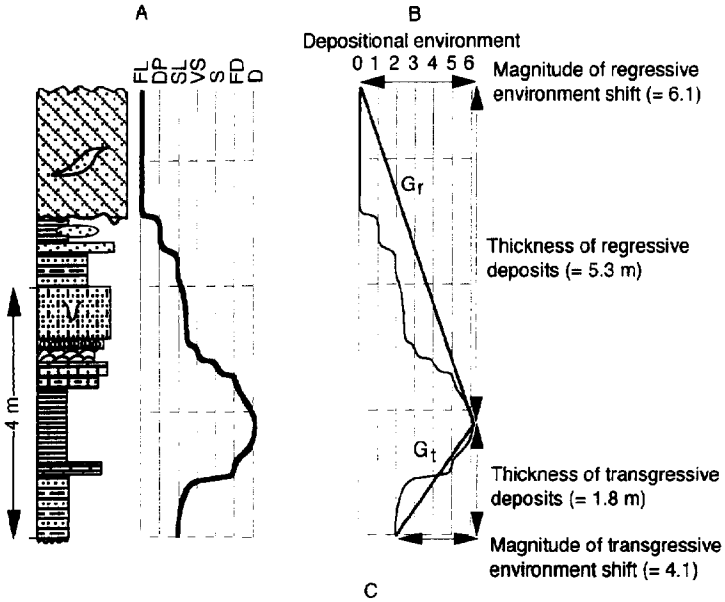

C

$$\text{Transg. stratigraphic environment gradient } (G_t) = \frac{\text{Magnitude of transg. environment shift}}{\text{Thickness of transgressive deposits}} = 2.28$$

$$\text{Reg. stratigraphic environment gradient } (G_r) = \frac{\text{Magnitude of reg. environment shift}}{\text{Thickness of regressive deposits}} = 1.15$$

$$\text{Cycle symmetry index} = \frac{\text{Reg. stratigraphic environment gradient } (G_r)}{\text{Transg. stratigraphic environment gradient } (G_t)} = 0.5$$

D

Cycle Symmetry	Asymmetrical	Symmetrical	Asymmetrical
Cycle SI	<1	1	>1
G_t and G_r	$G_r < G_t$	$G_r = G_t$	$G_r > G_t$

FIG. 6.—Attributes of a transgressive–regressive cycle. **A)** A measured section and environment interpretation as in Figure 5. **B)** Delineation of the magnitude of transgressive and regressive facies shifts, thickness of regressive and transgressive deposits, and transgressive and regressive stratigraphic environment gradients (G_t, G_r). Ranks of depositional environments are used in calculation of magnitude, gradient, and cycle symmetry index. **C)** Definitions of stratigraphic environment gradients and cycle symmetry index. Actual measurements are used to demonstrate the calculation of cycle symmetry index. **D)** Classification of cycle symmetry.

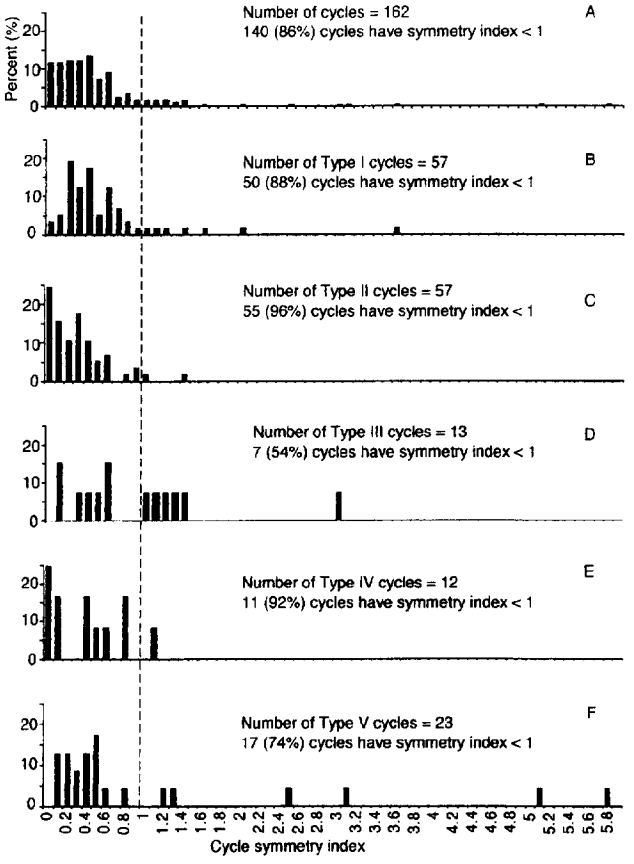

FIG. 7.—Symmetry index distribution of **A)** complete or nearly complete Cisco cycles, and **B–F)** lithologically defined cycle types. The dashed line indicates a symmetry index value of one. See Table 2 and Figure 8 for cycle classification.

sea-level rise and fall correspond to shoreline transgression and regression. This assumption is not true in many cases because shoreline movements are not solely controlled by eustatic sea-level changes (e.g., Sloss 1962; Curray 1964; Muto and Steel 1992; Leckie 1994). This can be demonstrated by varying model parameters. For example, regression can occur during an absolute sea-level rise if the depositional space at time t_0 (DS_0) is larger than that at time t_1 (DS_1) (Fig. 11). This requires that ($R_{r,sl} < R_{r,sed} - R_{r,sub}$), where $R_{r,sl}$ is rate of sea-level rise, $R_{r,sed}$ is rate of sedimentation, and $R_{r,sub}$ is rate of basement subsidence during the sea-level rise (Fig. 11). Transgression can occur during an absolute sea-level fall if the depositional space at time t_2 (DS_2) is larger than that at time t_1 (DS_1). This requires that ($R_{r,sl} < R_{r,sub} + R_{r,sub*} - R_{r,sed}$), where $R_{r,sl}$ is rate of sea-level fall, $R_{r,sub}$ is rate of basement subsidence, $R_{r,sub*}$ is rate of subsidence caused by compaction of contemporaneous sediments, and $R_{r,sed}$ is the rate of sedimentation during the sea-level fall (Fig. 11). It can also be demonstrated that shoreline transgression and regression are determined by the interplay between subsidence and sedimentation (or sediment supply) when absolute sea-level changes are fixed.

Cycle SI in thickness relates to cycle SI in time via regressive and transgressive sedimentation rates (Fig. 11). Cycle SI in time is the ratio between the rates of decrease of depositional space during regression and increase during transgression (Fig. 11). The rate of change of depositional space is explicitly determined by rates of sea-level change, sedimentation, and subsidence. Controls, such as climate, sediment yield, and sediment supply are implicitly included in the term for sedimentation rate. In the following, the formulated relations are used to explain the asymmetry of Cisco cycles as

TABLE 2.—*Cycle classification of the Cisco Group in outcrop.*

		Component lithofacies	Cycle types[b] I	II	III	IV	V
Regression	Maximum	Fluvial and delta-plain sandstones and shales	x	x	x	x	x
	Late	Marginal marine and deltaic sandstones and shales	x	x	x	x	x
		Shallow marine sandstones and shales	x	x	x	x	**X**
	Early	**Shallow marine carbonates**[a]	**X**	**X**	**X**		
Transgression	Maximum	**Fairly deep to deep marine core shales**	**X**		*	*	*
	Late	**Shallow to fairly deep marine carbonates**	**X**	**X**		**X**	
	Early	Shallow to marginal marine sandstones and shales	x	x	x	x	**X**
		Marginal marine and delta-plain nonmarine sandstones and shales	*	*	x	*	x

[a] Lithofacies in bold letters are principal lithofacies used to define cycle types.
[b] "**X**", the lithofacies which must be present in a certain type of cycles; "x", commonly present; "*", rarely present; "blank", not present.

the stratigraphic response to the systematic changes of these processes at the sub-cycle scale, and to demonstrate the potential predictive power of the relations in assessing the controls of these processes on cycle formation and architecture.

Symmetry of Controlling Processes

Cisco cycle asymmetry implies that the major controlling processes are not mirrored between the transgressive and regressive hemicycles. These processes are grouped into two categories: (1) the processes controlling accommodation space, such as base-level changes and basement subsidence; and (2) the processes controlling the volume and composition of sediments, such as climate, sediment yield, and sediment supply. Basement subsidence includes tectonic subsidence and subsidence induced by loading of water and sediment on the shelf and by compaction of the underlying sediments. These processes are mostly allogenic and operate on a regional scale. Some autogenic processes, such as those intrinsic to specific depositional or geomorphic environments, also contribute to changes in accommodation space and/or sedimentation. In the following sections, systematic variations of the allogenic processes are discussed in the context of cyclic sedimentation of the Cisco Group.

Sea-Level Variations.—Continental glaciation and deglaciation and eustatic sea-level fluctuations similar to those of the Plio-Pleistocene are documented for the late Paleozoic (e.g., Crowell 1978; Veevers and Powell 1987). Many studies of Pennsylvanian and Permian cyclic sequences have suggested a eustatic sea-level control on formation of transgressive–regressive cycles (e.g., Wanless and Shepard 1936; Wilson 1967; Heckel 1977, 1986; Goldhammer et al. 1994). Eustatic sea-level changes in the Eastern Shelf during Virgilian and Wolfcampian epochs have been suggested on the basis of large changes of paleo–water depth over a cycle interval (e.g., Lee 1938; Harrison 1973; Boardman and Malinky 1985; Aldis et al. 1988), inter-basinal correlation within the existing biostratigraphic framework (e.g., Boardman and Heckel 1989), and depositional sequence stratigraphic reconstruction of lowstand, transgressive, and highstand system tracts across the Eastern Shelf (Brown et al. 1990). In addition, cycle stacking patterns and spectral analysis of 30 Cisco sequences indicate presence of Milankovitch eccentricity, obliquity, and precessional index signals (Yang 1995). These studies suggest that glacio-eustatic sea-level changes of Milankovitch origin exerted direct control on the submarine accommo-

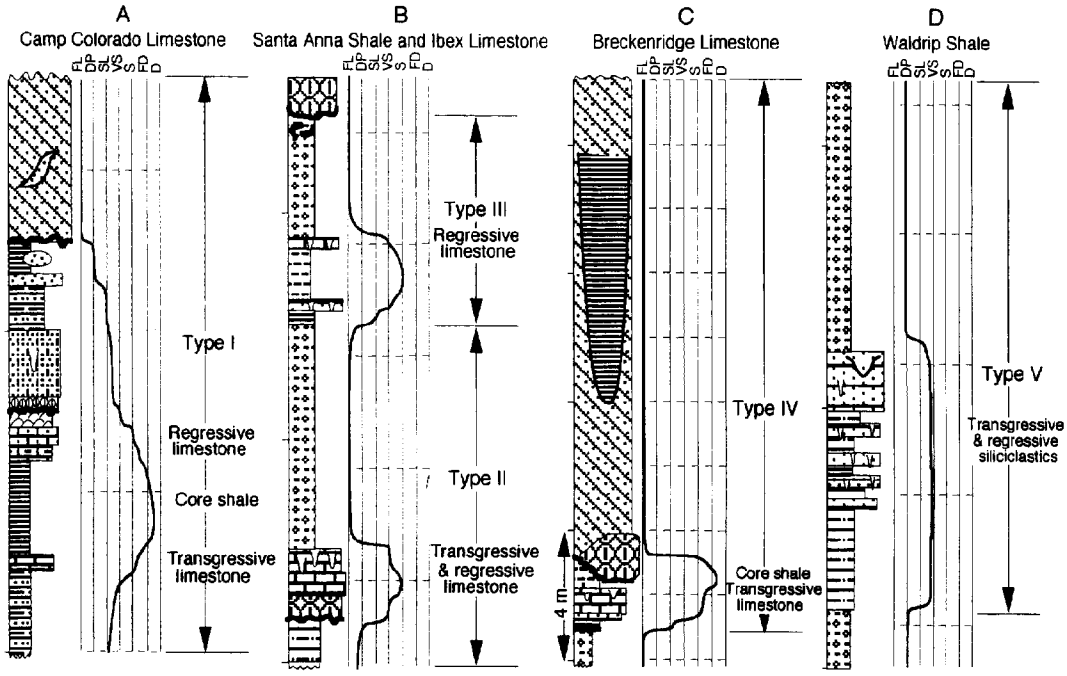

FIG. 8.—Simplified sections showing five cycle types: **A)** Type I; **B)** Types II and III; **C)** Type IV; and **D)** Type V. Section locations are shown in Figure 1. See Tables 1 and 2 for classification and descriptions of component lithofacies, and Figure 5 for keys.

dation space and sedimentation as well as major shoreline transgression and regression on the Eastern Shelf during Cisco time.

Thus, the symmetry of sea-level cycles in Cisco time may be analogous to that of the Plio-Pleistocene cycles. Rapid eustatic sea-level rises and slow falls during the Plio-Pleistocene have been documented from uplifted coral terraces (e.g., Cronin 1983; Chappell and Shackleton 1986); they are indicated by the shape of deep-sea oxygen isotope records (Williams 1988), and are consistent with modeling of dynamic continental ice melting and buildup (e.g., Imbrie and Imbrie 1980). The symmetry index of the Plio-Pleistocene sea-level cycles are calculated as (Fig. 11)

$$\text{Sea-level SI} = \frac{R_{r,sl}}{R_{t,sl}}$$

The SIs are calculated for cycles of ca. 100 k.y. and 20–40 k.y. duration, and for cycles located on the rising and falling limbs of ca. 100 k.y. cycles (Fig. 12). The majority of these sea-level cycles are asymmetrical, with a fast rise and a slow fall. Sea-level cycles of ca. 100 k.y. and those on the rising limbs are more asymmetrical in regard to both SI value and cycle abundance. The similar SI distribution between Plio-Pleistocene sea-level cycles and Cisco cycles suggests that eustatic sea-level changes significantly influenced the Cisco cycle symmetry (Fig. 12). Fast transgression and slow regression caused by fast eustatic sea-level rise and slow fall are suggested for the midcontinent Pennsylvanian cyclothems (Heckel 1984). This asymmetry probably also occurred during the Late Pennsylvanian and Early Permian on the Eastern Shelf, as suggested by the steep stratigraphic gradient of the transgressive deposits as compared to the shallow gradient of the regressive deposits (Fig. 13A).

Comparing the SI distributions of different types of Cisco cycles with those of different sea-level cycles reveals a similarity between Types II and IV cycles and ca. 100 k.y. sea-level cycles or those on the rising limbs of ca. 100 k.y. sea-level cycles, and between Type III cycles and sea-level cycles on the falling limbs of ca. 100 k.y. cycles (Figs. 7, 12). SIs of Types I and V cycles may be comparable with those of the 20–40 k.y. sea-level cycles or those on the falling limbs. The correlation is tentative in evaluating the origin of Cisco cycles, because cycle SI in thickness is not equal to the sea-level cycle SI in time (Fig. 11).

Subsidence Variations.—Basement subsidence is not constant over a cycle interval. It does not include subsidence induced by compaction of contemporaneous sediments. Net subsidence must have occurred over an observed cycle interval because basement subsidence is the ultimate control on sediment preservation. Tectonic subsidence can be regarded as constant over a cycle interval, whereas loading-induced subsidence is usually greater during regression than during transgression because, in general, thicker sediments are deposited during regression (Figs. 8, 10B). Sediment-loading-induced subsidence must lag behind loading, and the duration of this lag depends on the rigidity of basement rocks. If the lag is ignored by assuming instantaneous isostatic adjustment, basement subsidence is generally larger during regression than during transgression (Fig. 13A).

Basement subsidence rate, combined with the rate of absolute sea-level change, determines the symmetry of change in submarine accommodation space over a cycle interval, which is (Fig. 11)

$$\text{Accommodation SI} = \frac{(R_{r,sl} - R_{r,sub})}{(R_{t,sl} + R_{t,sub})}$$

If basement subsidence does not occur (i.e., $R_{r,sub} = R_{t,sub} = 0$), Eq 2 is the same as Eq 1, indicating that the accommodation symmetry is solely controlled by sea-level changes. If basement subsidence occurs (i.e., $R_{r,sub}$, $R_{t,sub} > 0$), the accommodation SI in Eq 2 is smaller than the sea-level SI in Eq 1. In other words, basement subsidence increases the accommodation asymmetry that is solely controlled by sea-level changes. Furthermore, a large subsidence rate during regression ($R_{r,sub}$) due to loading of thick regressive deposits accentuates the asymmetry by reducing the rate of decrease in accommodation space during regression (i.e., $R_{r,sl} - R_{r,sub}$). In the extreme, if the basement subsidence rate during regression is larger than the rate of sea-level fall, the accommodation space increases, rather

than decreases, during regression. In summary, accommodation asymmetry results in a faster increase in accommodation space during transgression and a slower decrease during regression.

Trends of changes in subaerial accommodation space on the Eastern Shelf are complex. The river gradient is determined by the horizontal distance and the relief between the headland and the shoreline. It decreases as the shoreline regresses on a very shallow shelf (Fig. 14A). Thus, regression results in elevation of the graded river profile, which caps the subaerial accommodation space, and causes an increase of accommodation space (Galloway, personal communication 1994). The river gradient starts to increase as the shoreline moves basinward of the shelf edge and descends on basin slope during maximum regression. Downshift of shoreline on the slope causes decrdase in subaerial accommodation space and channel downcutting on the up-dip part of the exposed shelf (Fig. 14A). Conversely, when the shoreline moves landward up the slope during early transgression, the river gradient decreases and the subaerial accommodation increases; continued transgression above the shelf edge results in an increasing river gradient and decreasing subaerial accommodation until the shoreline crosses the depositional site in the landward direction (Fig. 14A, B).

The Eastern Shelf is very shallow, dipping less than 1° westward (Fig. 3; Wermund and Jenkins 1969). The above scenario of changes in river gradient and subaerial accommodation is applicable to this shelf. The increase in subaerial accommodation space during late regression further slows the overall decrease in accommodation space during regression (Fig. 14). A slow decrease in accommodation space allows room and time for sediments to aggrade, resulting in a great aggradational component in the generally progradational regressive sediment package. In contrast, a fast increase in accommodation during transgression tends to cause sediment starvation in the generally retrogradational transgressive package (Brown et al. 1990; Yang 1995).

The sediment surface is above the basement surface or the top of the underlying cycle. Therefore, subsidence of the sediment surface due to compaction of contemporary sediments in the present cycle (i.e., R_{sub^*} in Figure 11) is not a factor in Eq 2. It does not affect the accommodation space because accommodation space is defined as the distance between base level and the top of the underlying cycle.

Climatic Variations.—Intra-cycle climatic variations in precipitation seasonality and the amount of annual precipitation are of interest to this study. They greatly affect erosion rate and sediment production in the upland source areas, transportation capacity of streams from source areas to the depositional site, and sediment characteristics.

The Eastern Shelf was located in the equatorial wet belt during the Virgilian and Wolfcampian epochs as the southwestern United States migrated from the Southern Hemisphere to the Northern Hemisphere during Early Carboniferous to Permian time (Fig. 4; Witzke 1990). It underwent a low-latitude glacial–interglacial climate. The climate varies from a weakly seasonal, subhumid climate of long-wet/short-dry annual cycles during interglacials or transgression, to a highly seasonal climate of wet-dry annual cycles during interglacial–glacial transition or maximum transgression, and to a weakly seasonal, semiarid climate of short-wet/long-dry annual cycles during glacials or regression (Fig. 13B; Cecil 1990; Bull 1991; Tandon and Gibling 1994). The climate was probably also controlled by local rain-shadow effects, because the Eastern Shelf was surrounded by orographic highs to the north, east, and south (Fig. 1).

Intra-cycle climatic changes are interpreted from climate-sensitive lithofacies (e.g., Schutter and Heckel 1985; Cecil 1990; Tandon and Gibling 1994). A long-wet/short-dry, subhumid climate during early transgression is indicated by hydromorphic paleosols, such as lignite, carbonaceous shale, and associated leached paleosols, such as flint clay and underclay (Fig. 15A, B; Table 1; Cecil 1990; Tandon and Gibling 1994). A long-dry/short-wet, semiarid climate during late regression is indicated by well-developed, single-story or multistory vertisols, and calcic/clayey nodules in the upper regressive siliciclastic deposits, abundant coated carbonate grains such as *Osagia*, and some brackish-water carbonates in the upper regressive limestones (Fig. 15C, D, E). A highly seasonal, wet-dry climate transitional between subhumid and semiarid is postulated for the period of maximum transgression based on the model of Cecil (1990) (Fig. 13B). It can only be interpreted indirectly from the high influx of siliciclastics during late regression, which was probably mainly produced under a wet-dry climate during maximum transgression (see discussions below). Any direct nonmarine climatic indicators that were deposited in landward locations are not preserved.

Virgilian and Wolfcampian climatic variations in the Eastern Shelf are less extreme than the Carboniferous climate of the eastern United States, which ranges from nonseasonal tropical rainy to semiarid-arid (Cecil 1990). Coal beds in Cisco cycles are thin, planar, and discontinuous, and commonly composed of sandy lignites or highly carboniferous shales. These coals are different from the thick minable coals deposited in a tropical rainy climate in the Carboniferous of the Appalachian Basin (Cecil 1990). In addition, the Cisco regressive deposits commonly contain locally concentrated calcic and clayey nodules, and well-developed vertisols, but not well-developed layers of calcretes and evaporites, and aridisols as in the Appalachian Basin (Table 1; Cecil 1990). These features indicate a semiarid, rather than arid, climate. Inter-cycle climatic variations are also suggested by some cycles containing neither hydromorphic nor calcareous paleosols.

Glacial to interglacial climatic variations are linked to eustatic sea-level changes on the basis of stratigraphic repetition of climate-sensitive lithofacies and their respective positions within transgressive–regressive cycles, which are demonstrated to be controlled by glacio-eustatic sea-level changes (e.g., Schutter and Heckel 1985; Cecil 1990; Tandon and Gibling 1994; Soreghan 1994; and Quaternary analogs referenced therein). Cecil (1990) suggested that late Paleozoic climate cycles of the Appalachian Basin were caused by Milankovitch orbital variations in eccentricity, obliquity, and precession, linking high-latitude glaciation and deglaciation to low-latitude seasonality and variations in precipitation. Tandon and Gibling (1994) explicitly linked a relatively humid climate to sea-level highstand hydromorphic paleosols and a relatively arid climate to lowstand and early-transgressive calcareous paleosols in Upper Carboniferous cyclothems. Their interpretation is substantiated by Quaternary analogs of climatic controls on formation of subhumid peats and semiarid calcretes and vertisols. Expansion and contraction of the intertropical convergence zone associated with deglaciation and glaciation during the latest Quaternary induced changes in precipitation from very humid to subhumid, or humid to dry conditions (Perlmutter and Matthews 1989). Similar mechanisms for intra-cycle alternation of lowstand semiarid and highstand subhumid conditions are invoked to explain the cyclostratigraphy of the Pennsylvanian equatorial Pedregosa and Orogrande basins (Soreghan 1994).

The geometry of sea-level lowstand paleo-valleys incising adjacent interfluve vertisols observed by Tandon and Gibling (1994) is common in the Cisco Group (Fig. 8A, B, C; see also Brown 1960, 1962; Brown et al. 1990; Harrison 1973; Yang 1995). Consistent presence of subhumid hydromorphic paleosols in early-transgressive deposits and semiarid calcareous paleosols in maximum-regressive deposits in many Cisco cycles suggests systematic climatic variations corresponding to specific stages of transgression and regression. Climate probably varied from weakly seasonal subhumid in early and late transgression, to highly seasonal wet-dry during maximum transgression, and to weakly seasonal, semiarid during late and maximum regression (Fig. 13A, B).

Variations in Sediment Yield and Sediment Supply.—Sediment yield is the volume of earth materials yielded per unit area of drainage basin per unit time (Bull 1991), which will eventually be delivered to the depositional site. It is mainly controlled by the climatic regime, vegetation cover, bedrock lithology, and topography of the source areas (Schumm 1968; Wilson 1973). In modern catchment basins, maximum erosion, and therefore maximum clastic sediment yield, occur in climates of strong precipitation sea-

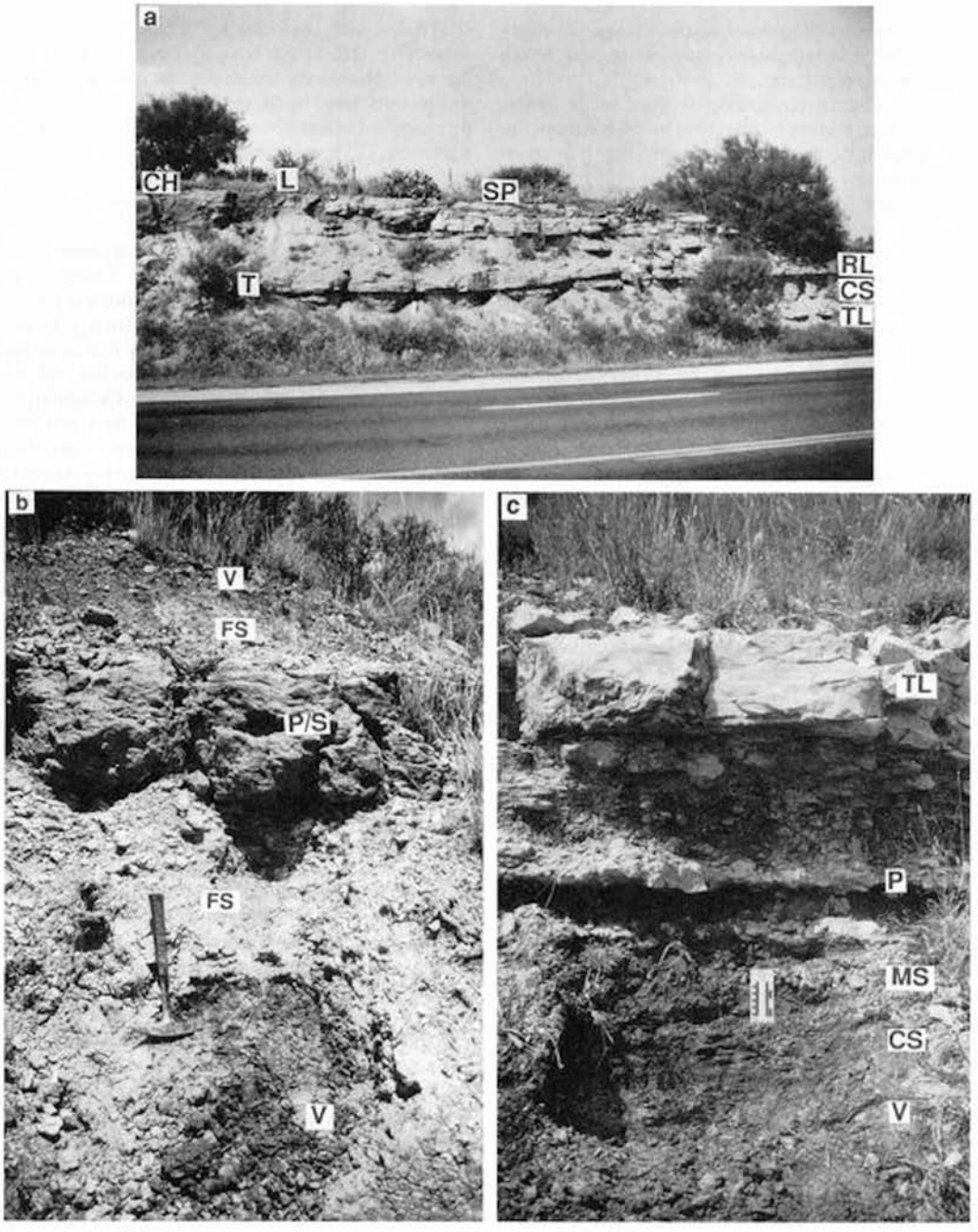

FIG. 9.—Features of the Cisco cycles. **A)** A Type I cycle with a maximum-regressive fluvial channel (CH) downcutting the entire cycle to the left in the Camp Colorado Limestone. The lower cycle boundary is not exposed. CS, maximum-transgressive core shale; L, fluvial levee sandstone; RL, regressive limestone; SP, crevasse-splay sandstone; T, tidal-channel sandstone; TL, transgressive limestone. Person is ~ 1.6 m tall. The measured section is shown in Figure 8A. **B)** A Type II cycle of the Salt Creek Bend Shale, with a fossiliferous shale (FS) in the lower part, which is in sharp contact with a vertisol (V) of the previous cycle, and grades into the overlying arenaceous packstone or skeletal sandstone (P/S). The packstone is highly burrowed at top and overlain by a 40-cm-thick fossiliferous marine shale (FS). The upper part is a 4-m-thick variegated vertisol (V) with abundant calcrete nodules. Hammer is 40 cm long. **C)** The transgressive interval of a Type I cycle of the Salt Creek Bend Shale. An undulating surface separates a pale gray, blocky vertisol (V) of the previous cycle from the carbonaceous and calcareous marginal marine shale (CS), which grades upward into a dark gray, calcareous, crinoid and bryozoan marine shale (MS). Upward-increasing arenaceous packstone lentils (P) are burrowed and highly fossiliferous. The wavy and thin transgressive limestone (TL) has abundant horn corals. **D)** A regressive fluvial channel complex consisting of channel sandstone (CH), mud-plug shale (MP), and crevasse-splay sandstone (SP), and overlying a thin transgressive limestone (TL). The regressive limestone and core shale are eroded at this location and reappear approximately 100 m to the left. Person is ~ 1.5 m tall. The measured section is shown in Figure 8C. **E)** A single, dense bed of upward-deepening transgressive packstone of the Bunger Limestone. The lower 10 cm is a well current-laminated packstone, the middle part is faintly laminated, and the upper part is bioturbated to current-laminated. The packstone is moderately arenaceous and very fossiliferous, including trilobites, brachiopods, echinoderms, bryozoans, crinoids, and other normal marine invertebrate fossils. Hammer is 40 cm long. **F)** Upward-shallowing regressive packstone to wackestone of the Lower Gunsight Limestone. A trend of upward-increasing meteoric alteration, limonite replacement, and burrowing is observed. Large (~ 10 cm long) horn corals dominate in the argillaceous lower part, phylloidal algae dominate in the arenaceous upper part. The lower and upper contacts are gradational. Beds become thinner and more discontinuous upward, and geopetal structures become common. Stick is 1 m long. See Figure 1 for locations.

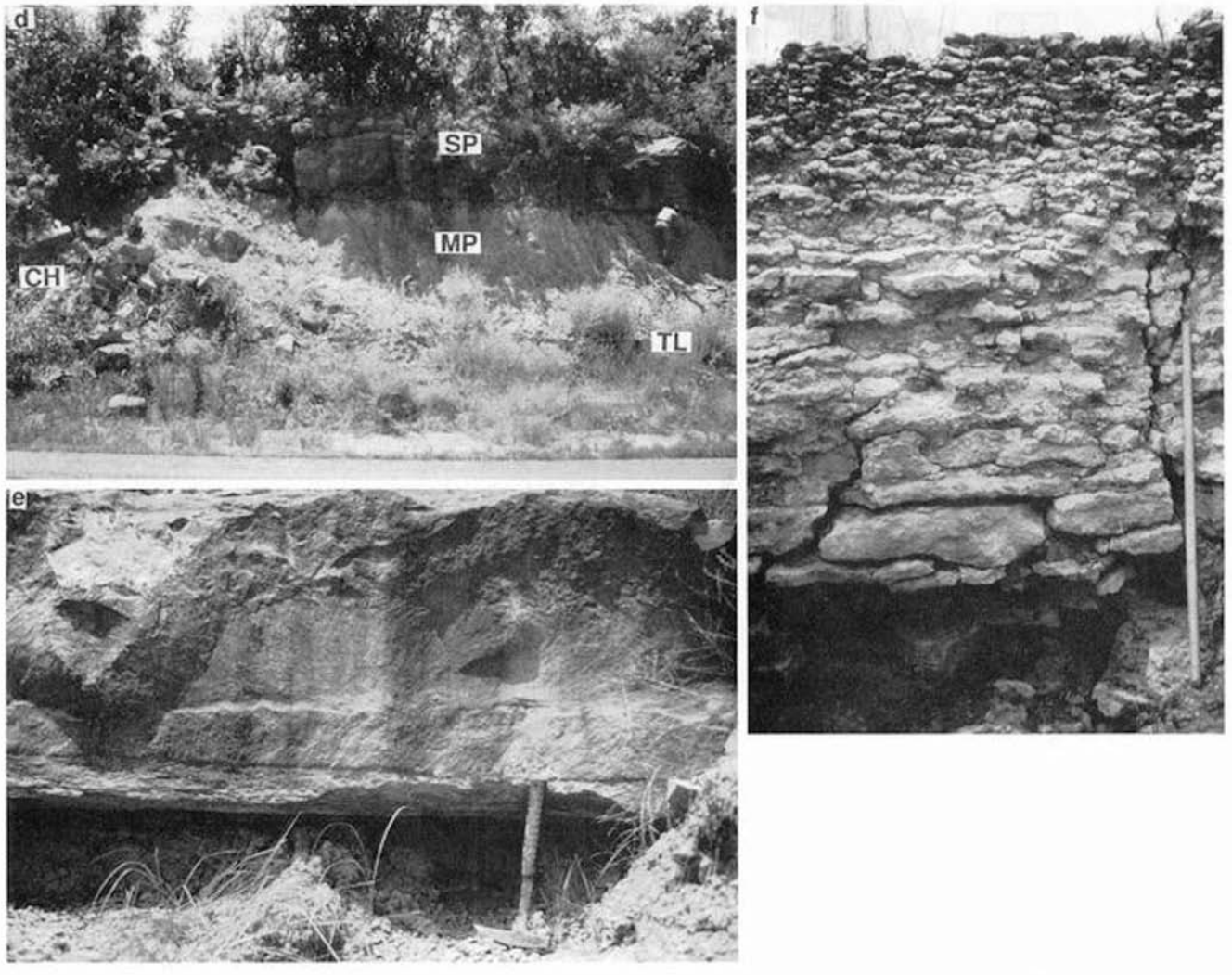

FIG. 9.—Continued.

sonality, especially wet-dry climates (Wilson 1973; Cecil 1990). Schumm (1968) predicted that the climatic condition for peak sediment production in drainage basins may shift from semiarid with annual precipitation of ~ 250–400 mm in Quaternary time to subhumid with annual precipitation of ~ 500–1000 mm between Devonian and Permian time, when vegetation cover was primitive and confined in coastal plains and humid valleys. According to Schumm's (1968) prediction (see also Wilson 1973 on relation between seasonality and erosion), erosion and sediment yield in the upland in Cisco time probably increased with intensified precipitation in the early and late transgression, peaked under highly seasonal wet-dry climate around maximum transgression, and reached the minimum in the late and maximum regression (Fig. 13B).

Sediment supply is the volume of sediments delivered to the depositional site per unit time. It is mainly determined by stream transportation capacity, vegetation cover, topographic relief between the source and depositional site, and sediment yield. Wilson (1973) pointed out that variations in sediment supply depend more on sediment yield than on sediment transport. Peaks of sediment yield in source areas and sediment supply at depositional sites likely are out of phase because of temporary sediment storage in drainage basins and coastal plains. The phase difference is mainly determined by the type and size of storage, distance and relief between the source and depositional site, vegetation cover, and valley slope stability (Schumm 1968). During deposition of the Cisco cycles, limited sediment supply during transgression is indicated by thin, nonmarine and marginal marine siliciclastics, and copious supply during regression is indicated by thick, coastal-plain and fluvial siliciclastics, which constitute the major part of Cisco cycles (Figs. 9A, C, D, 10B; Table 1). Thus, for the Cisco cycles, peak sediment yield occurred around maximum transgression, but peak sediment supply occurred during the late and maximum regression; as a result, peak sediment yield lags behind peak sediment supply by approximately a half cycle (Fig. 13B).

Sediment storage during transgression is the key to understanding the lag between sediment yield and sediment supply. Two types of sediment sinks are recognized during the Holocene marine transgression. First, coastal-plain topographic lows trap sediments because of a littoral energy fence formed by transgressing sea water (Swift and Thorne 1991). In the Alabama Gulf of Mexico coastal zone, rapid Holocene transgression inundated the present continental shelf and developed a barrier

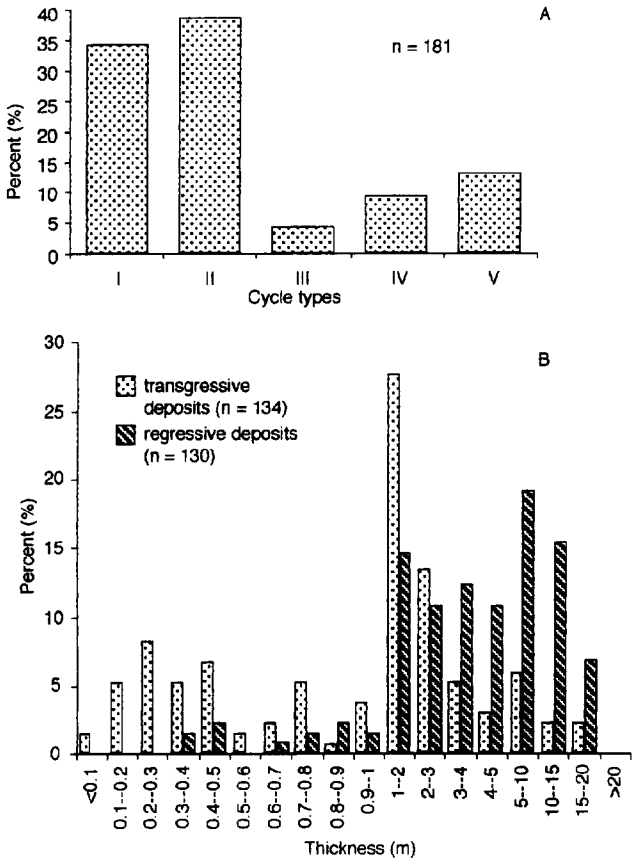

FIG. 10.—A) Distribution of five types of transgressive–regressive cycles. Each cycle is a sample. 181 cycles are from all the measured sections. B) Thickness distribution of complete transgressive and regressive deposits in the Cisco Group.

and lagoon complex around Mobile Bay (Davies and Hummell 1994). The bay acted as a sink for aggrading bay/lagoonal muds and muddy sands from the Mobile River during late transgression (Davies and Hummell 1994). This is probably analogous to sediment trapping in coastal plains and estuaries during the Cisco transgressions. Fast transgression or shelf deepening, caused by fast sea-level rise and enhanced by a shallow shelf profile during early transgression, walled off much clastic influx onto the shelf and did not allow enough time for sediments to fill the shelfal accommodation space.

The second sediment sink is floodplains and river valleys in the drainage basins. Blum et al. (1994) documented the Quaternary climatic controls on sediment removal and storage in the Colorado River drainage basin of Texas. The balance between sediment yield and stream power determines the volume of sediment removal or storage. Subhumid climate produces more sediments and greater stream power than semiarid climate, but sediment yield exceeds stream transportation capacity, resulting in alluvial deposition. Floodplain construction by vertical accretion was significant when moist climatic conditions prevailed and relatively frequent basinwide precipitation events acted on exposed bedrock landscapes (Blum et al. 1994). Sediment removal from the drainage basins likely occurs during semiarid climate because of relatively large transportation capacity of frequent flash floods (Blum et al. 1994).

This mode of sediment storage and removal was probably very important for the Cisco cycles. Limited primitive vegetation cover and subhumid climate in the upland facilitated sediment production during transgression. Sediments shed from poorly vegetated hill slopes and from tributary channels could have been stored in main valleys through the stabilizing effects of vegetation (Schumm 1968). Weakened vegetation cover under drier climate during regression would have promoted removal of these stored sediments. High sediment influx, resulting from sediment removal from drainage basins, overcame the sea-water barrier, filling a large regressive accommodation space at the depositional site (Fig. 13A, B).

Sediment-supply symmetry at the depositional site over a cycle interval can be expressed as

$$\text{Sediment-supply SI} = \frac{R_{r,sed}}{R_{t,sed}} \tag{3}$$

$$= \frac{T_r t_t}{T_t t_r} \tag{4}$$

where T_r and T_t are the thickness of regressive and transgressive deposits, and t_t and t_r are the duration of transgression and regression. Sediment supply SI can be approximated by the ratio of T_r to T_t, which is larger than the real sediment supply SI because t_t/t_r is likely smaller than one. About 82% of Cisco cycles have approximated sediment supply SIs larger than one, and more than 60% have regressive sediment supply that is more than two times larger than the transgressive supply (Fig. 16).

Cycle Symmetry and Controlling Processes

Accommodation space and sediment supply control depositional space at the depositional site, which is the distance between the sediment surface and base level (Figs. 11, 13C). The control of sediment supply on depositional space includes sediment infilling of accommodation space and compaction of contemporary sediments (Fig. 11). Thick regressive deposits cause larger loading- and compaction-induced subsidence than thin transgressive sediments. Roberts et al. (1994) showed that the subsidence rate of the coastal plains of the Mississippi River Delta increases directly with the thickness of underlying Holocene deposits. The increase in subsidence rate must be the combined effect of increased sediment loading and compaction assuming a constant regional basement subsidence. Based on this analog, subsidence of the sediment surface on the Eastern Shelf would have been accelerated by loading and compaction of thick regressive sediments to slow the rate of decrease of depositional space.

Depositional space in marine environments is equal to paleo-water depth, which is the basis for ranking marine depositional environments for the Cisco cycles. Thus, the ratio of regressive to transgressive depositional space changes is the cycle symmetry in time (Fig. 11):

$$\text{Cycle SI in time} = \frac{(R_{r,sl} + R_{r,sed.marine} - R_{r,sub} - R_{r,sub^*})}{(R_{t,sl} - R_{t,sed.marine} + R_{t,sub})} \tag{5}$$

Cycle SI in time is larger than the accommodation SI (Eq 2) because R_{r,sub^*} is smaller than $R_{r,sed,marine}$, the sedimentation rate of regressive marine sediments before compaction.

Cycle symmetry in thickness can be derived as (Fig. 11):

$$\text{Cycle SI in thickness} = \text{Cycle SI in time} \cdot \frac{R_{t,sed.marine}}{R_{r,sed.marine}} \tag{6}$$

Assuming a constant sedimentation rate ($R_{t,sed,marine} = R_{r,sed,marine}$), cycle symmetry in thickness is the same as that in time. However, the sedimentation rate of generally finer-grained transgressive deposits is probably slower than that of generally coarser-grained regressive sediments. Therefore, $(R_{t,sed,marine})/(R_{r,sed,marine})$ is smaller than one, and cycle SI in thickness is smaller than cycle SI in time. In other words, cycle SI in thickness overestimates the asymmetry of Cisco cycles in time.

Consideration of subaerial depositional space, which is the distance between sediment surface and the graded river profile, complicates cycle SI in Eq 5. One can envision a single concave-upward base level composed

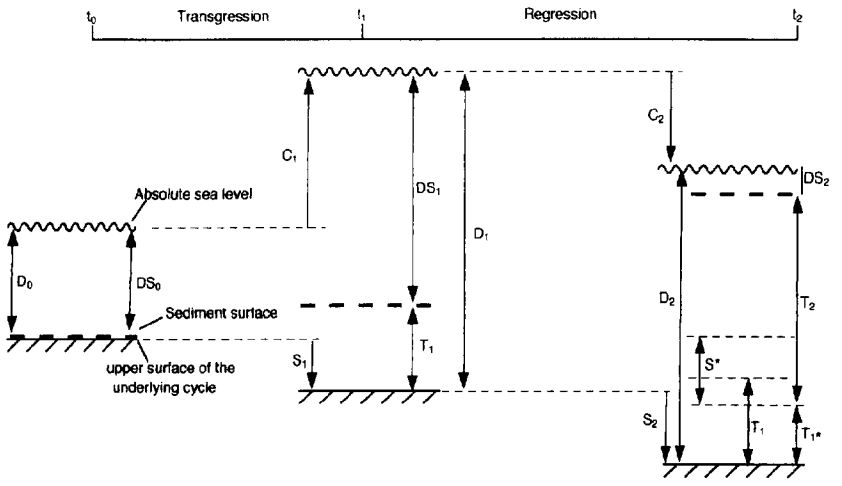

Sea level	0	C_1	C_2
Subsidence	0	S_1	S_2
Sediment thickness	0	T_1	$T_{1*} + T_2$
Accommodation	D_0	$D_1 = D_0 + C_1 + S_1$	$D_2 = D_1 + S_2 - C_2$
Depositional space	DS_0	$DS_1 = DS_0 + C_1 + S_1 - T_1$	$DS_2 = DS_1 + S_2 + S^* - C_2 - T_2$

Sea-level gradient (or rate): $G_t = (C_1)/(t_1 - t_0)$; $G_t = (C_2)/(t_2 - t_1)$

Accommodation gradient: $G_t = (D_1 - D_0)/(t_1 - t_0) = (C_1 + S_1)/(t_1 - t_0)$; $G_r = (D_1 - D_2)/(t_2 - t_1) = (C_2 - S_2)/(t_2 - t_1)$

Stratigraphic environment gradient in time: $G_t = (DS_1 - DS_0)/(t_1 - t_0) = (C_1 + S_1 - T_1)/(t_1 - t_0)$; $G_r = (DS_1 - DS_2)/(t_2 - t_1) = (C_2 + T_2 - S_2 - S^*)/(t_2 - t_1)$

Stratigraphic environment gradient in thickness: $G_t = (C_1 + S_1 - T_1)/(T_1)$; $G_r = (C_2 + T_2 - S_2 - S^*)/(T_2)$

Sea-level symmetry index = $\{(t_1 - t_0)/(t_2 - t_1)\} \cdot (C_2/C_1) = (R_{t,sl})/(R_{r,sl})$

Accommodation symmetry index = $\{(t_1 - t_0)/(t_2 - t_1)\} \cdot \{(C_2 - S_2)/(C_1 + S_1)\} = (R_{t,sl} - R_{t,sub})/(R_{r,sl} + R_{r,sub})$

Cycle symmetry index in time = $\{(t_1 - t_0)/(t_2 - t_1)\} \cdot \{(C_2 + T_2 - S_2 - S^*)/(C_1 + S_1 - T_1)\} = (R_{t,sl} + R_{t,sed} - R_{t,sub} - R_{t,sub*})/(R_{r,sl} - R_{r,sed} + R_{r,sub})$

Cycle symmetry index in thickness = $(T_1)/(T_2) \cdot \{(C_2 + T_2 - S_2 - S^*)/(C_1 + S_1 - T_1)\} = (\text{Cycle SI in time}) \cdot (R_{t,sed})/(R_{r,sed})$

FIG. 11.—Diagram showing major processes and geometry in creation and infilling of accommodation space in a shallow shelf setting during transgression and regression, and derivation of symmetry indices of sea level, accommodation, and transgressive–regressive cycles. For simplicity, base level is depicted as the absolute sea level. The variables used in the diagram are designated as follows. C = amplitude of absolute sea-level change. It is always positive. D = accommodation space. It can be negative. DS = depositional space. It can be negative. S = subsidence induced by tectonics and loading of water and sediment on the basement and by compaction of underlying sediments. To ensure positive symmetry indices, sea level, accommodation, and stratigraphic environment gradients are always positive. Notations used in the diagram are defined as: $R_{t,sl}$, $R_{r,sl}$ = rates of sea-level changes; $R_{t,sed}$, $R_{r,sed}$ = rates of sedimentation; $R_{t,sub}$, $R_{r,sub}$ = rates of basement subsidence; $R_{r,sub*}$ = rate of subsidence due to compaction of contemporary sediments; S^* = subsidence due to compaction of contemporary transgressive and regressive sediments; t_0, t_1, t_2 = time points; T_1, T_2 = original sediment thickness before compaction; T_{1*} = thickness of transgressive deposits after contemporary compaction; 0, 1, 2 = subscripts corresponding to time points t_0, t_1, and t_2; *sed* = subscript for sedimentation; *sl* = subscript for sea level; *sub* = subscript for subsidence; *t*, *r* = subscripts for transgressive and regressive stages.

of two segments tied at the shoreline, the absolute sea level seaward of the shoreline and the graded river profile landward of the shoreline (Fig. 14A). In the up-dip part of the Eastern Shelf, base level is the lowering sea level during regressive marine sedimentation; it switches to an elevating graded river profile during regressive marginal-marine and nonmarine deposition and, finally, to a lowering river profile during maximum-regressive nondeposition and erosion. An opposite trend should characterize the period of early transgression (Fig. 14B).

$R_{r,sl}$ and $R_{t,sl}$ in Eq 5 can be changed to $R_{r,baselevel}$ and $R_{t,baselevel}$ to take into account changes in subaerial depositional space, where $R_{r,baselevel} = R_{r,rp} + R_{r,sl}$ and $R_{t,baselevel} = R_{t,rp} + R_{t,sl}$, where $R_{r,rp}$ and $R_{t,rp}$ are the rates of graded river profile changes during regression and transgression. In this case, base-level elevation does not decrease or increase uniformly during regression or transgression. Nonetheless, the net change of base level over the entire period of regression or transgression is one of lowering during regression and of rising during transgression.

$R_{r,rp}$ and $R_{t,rp}$, however, are difficult or impossible to estimate from the stratigraphic record. Practically, the thickness of nonmarine deposits can be used to approximate the subaerial depositional space and, thus, sedimentation rates of transgressive and regressive nonmarine deposits ($R_{t,sed,nonmarine}$, $R_{r,sed,nonmarine}$) are used to replace $R_{r,rp}$ and $R_{t,rp}$. This approximation conforms with the calculation of SIs of the Cisco cycles. In this case, ($R_{t,baselevel} - R_{r,baselevel}$) is smaller than ($R_{t,sl} - R_{r,sl}$) because $R_{t,sed,nonmarine}$ is likely smaller than $R_{r,sed,nonmarine}$. Therefore, according to Eq 5, cycle asymmetry decreases with consideration of subaerial sedimentation.

Cycle symmetry index in time for cycles composed of nonmarine and marine deposits can be derived by substituting $R_{t,sl}$ and $R_{r,sl}$ for $R_{t,baselevel}$ and $R_{r,baselevel}$ in Eq 5:

$$\text{Cycle SI in time} = \frac{(R_{t,sl} + R_{t,sed,marine} + 2{\cdot}R_{t,sed,nonmarine} - R_{t,sub} - R_{t,sub*})}{(R_{t,sl} - R_{t,sed,marine} + 2{\cdot}R_{t,sed,nonmarine} + R_{t,sub})} \quad (7)$$

Eq 7 establishes a relation between stratigraphic response (i.e., cycle SI) and rates of controlling processes. It indicates that cycle symmetry reflects the balance between processes controlling accommodation and those controlling sediment infilling during transgression and regression. In other words, cycle SI is an indicator of the relative dominance of these two groups of processes during transgression and regression.

The roles of sediment infilling versus accommodation can be explored using Eq 5, to demonstrate the potential predictive power of this relation. For example, an increase in transgressive supply ($R_{t,sed}$) and/or in regressive accommodation ($R_{r,sl} - R_{r,sub}$) makes cycle SI closer to one or a cycle more symmetrical. Transgressive sediment supply ($R_{t,sed}$), however, has a

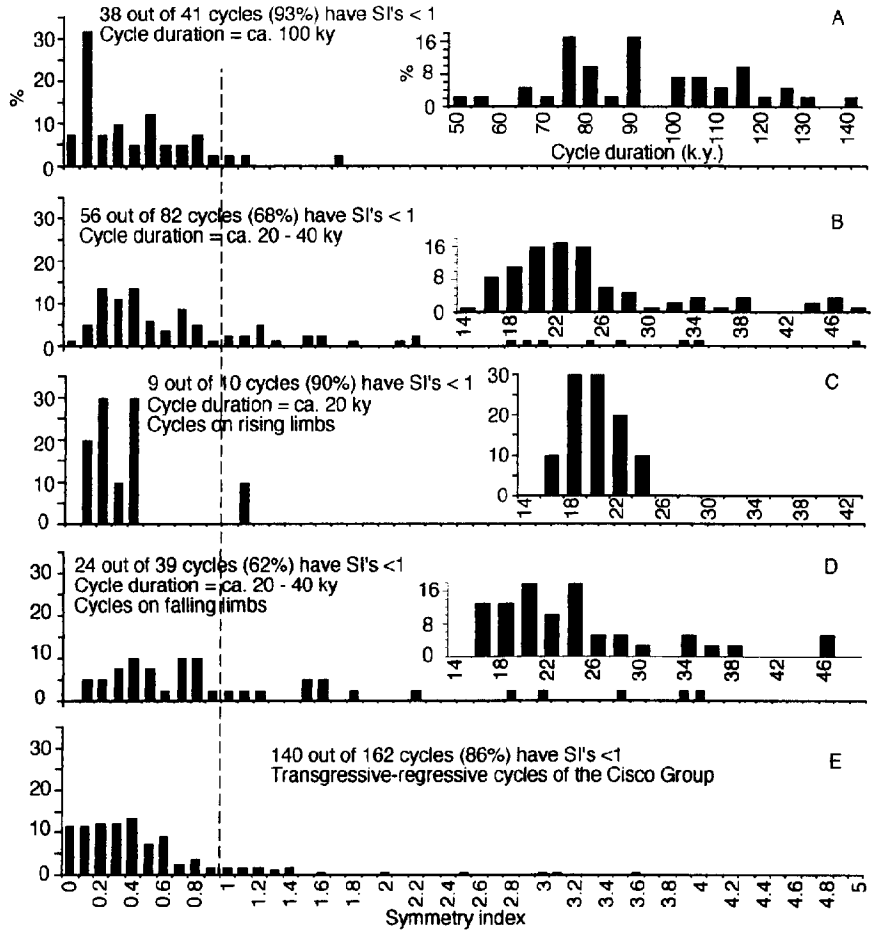

FIG. 12.—Distribution of symmetry index in time of Plio-Pleistocene sea-level cycles. Durations of these cycles span ca. **A)** 100 k.y. and **B)** 20–40 k.y. The cycles are on the **C)** rising limb and **D)** falling limb of ca. 100 k.y. cycles. **E)** Distribution of symmetry index in thickness of the Cisco cycles is included for comparison. Insets show the duration distribution of cycles used in the calculation. The dashed line indicates symmetry index value of one. Used in the calculation are sea-level and oxygen-isotope cycles documented from uplifted coral terraces and deep-sea cores for the last 130 k.y. (Chappell and Shackleton 1986), deep-sea oxygen-isotope cycles from 120 k.y. to 900 k.y. BP (Bassinot et al. 1994) and from 900 k.y. to 1.8 my BP (Williams et al. 1988), and ice-volume cycles for the last 900 k.y. (Imbrie and Imbrie 1980).

decreasing trend, which is exaggerated by increasing transgressive accommodation. Regressive accommodation ($R_{r,sl} - R_{r,sub}$) also has a decreasing trend, which is exaggerated by increasing regressive sediment supply (Fig. 13A, B). Therefore, in the up-dip part of the Eastern Shelf, transgressive sedimentation is sediment-supply-controlled, whereas regressive sedimentation is accommodation-controlled (Fig. 13; see also Swift and Thorne 1991). These conditions determine the asymmetrical nature of the Cisco cycles. They also determine a retrogradational and aggradational depositional style for transgressive sedimentation and an aggradational and progradational style for regressive sedimentation, as signified by contrasting transgressive and regressive stratigraphic gradients.

MECHANISMS OF AUTOGENIC CONTROLS ON CYCLE CHARACTERISTICS

Formation of Cisco cycles is controlled not only by the allogenic processes discussed above but also by additional allogenic and autogenic processes, which may not operate in a regular pattern. Autogenic processes are probably not the major controls on Cisco cycle symmetry, but cause variations of some systematic trends.

Local topography, tectonics, and depositional dynamics result in erratic deviations from general trends of intracycle climatic, sea-level, subsidence, and sediment-supply changes, as indicated by intracycle and intercycle variations in sedimentary characteristics (e.g., Brown 1969; Galloway and Brown 1972; Yang 1995). Absence of regressive calcareous paleosols and/or nonmarine transgressive deposits, and conformable cycle boundaries, indicate intercycle variations in the magnitude of climate and sea-level changes. The magnitude variation is also indicated by the absence of maximum-transgressive core shale in more than 60% of cycles. The absence of transgressive limestones in Type III cycles, regressive limestones in Type IV cycles, and any limestones at all in Type V cycles may have been caused by local high clastic influx due to local variations in climate and/or tectonics. Common, but laterally nonpersistent, multistory paleosols in regressive deposits and rare limestone tempestites in core shales suggest episodic sedimentation and/or erratic climatic variations (Table 1; Yang 1995). The impact of local topography and depositional dynamics is substantiated by local lateral changes of cycle type, magnitude, and thickness as well as cycle disappearance in the Cisco Group (Fig. 17).

Transgressive and regressive limestones have similar faunal content and distribution of rock types (Yang 1995). But the upper regressive limestones commonly contain nonskeletal grainstone and supratidal carbonate composed of highly abraded and/or meteorically altered allochems (Fig. 15D–F; Table 1). In contrast to the generally thin, laterally persistent transgressive limestones, regressive limestones are thick, show frequent lateral thickness and facies changes, and in some cases are partly or entirely eroded (Figs. 8C; 9E, F). These characteristics indicate prolonged, "catch-up" and "give-up" regressive carbonate deposition in gradually shallowing environments, and short-lived "give-up" transgressive deposition in rapidly deepening environments. Conditions intrinsic to carbonate depositional environments, such as energy, oxygenation, substrate, and light penetration, are the major controls on texture, thickness, and facies distribution of the limestones (Yang 1995; see also Heckel 1984).

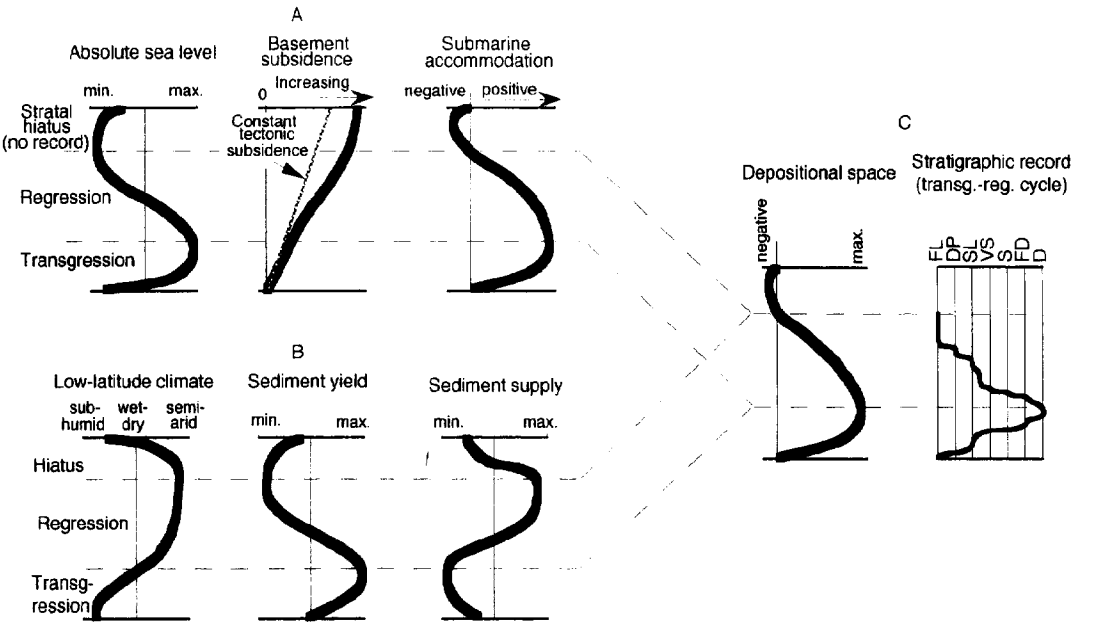

FIG. 13.—Systematic variations of allogenic processes controlling **A)** accommodation space and **B)** sediment infill. These trends are interpreted from stratigraphic and sedimentary characteristics of Cisco cycles (Table 1) based on existing models cited in the text. **C)** cycle asymmetry in time and thickness results from the combined effects of processes shown in **A** and **B.** No scale is intended. Vertical axes are in time in **A** and **B,** and for the depositional space in **C**; the stratigraphic record is in thickness.

Many limestones are contaminated with siliciclastics, forming a full spectrum of mixed lithologies, such as arenaceous packstone to calcareous sandstone, and argillaceous wackestone to calcareous shale (Brown 1960; Tierrie 1960; Yang 1995; Table 1). "*In situ* mixing" of carbonate-secreting organisms living in or being washed into clastic environments and "facies mixing" of siliciclastics and carbonates in transitional facies belts were the major autogenic mechanisms for lithologic mixing of the Cisco sediments within a largely depth-controlled facies mosaic on the Eastern Shelf (e.g., Lee 1938; Brown 1962; Harrison 1973; Yancey 1991; Yang 1995; see Mount 1984 for mechanisms of carbonate-siliciclastic mixing). Regionally, many limestones become thinner and impure toward clastic sources to the north and east, suggesting regional paleogeographic control on carbonate composition (e.g., Brown 1960, 1962; Yang 1995). Considerable lateral thickness and facies changes of regressive limestones resulted mainly from local clastic influx and shelf topography, both of which affect carbonate productivity and environments, in addition to postdepositional erosion and diagenesis.

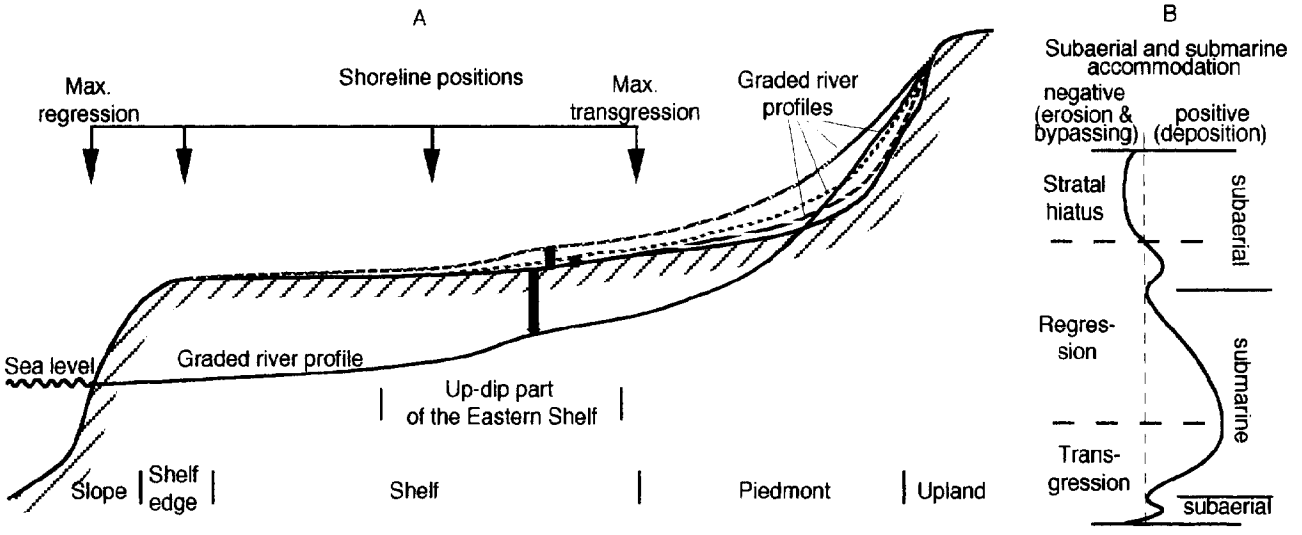

FIG. 14.—**A)** Changes of a river gradient as the shoreline migrates on a very shallow shelf. During early and late regression, subaerial accommodation space capped by the graded river profile on the shelf and outer piedmont increases when shoreline moves from the most landward position at maximum transgression to the shelf edge, as indicated by the two thick arrows above the shelf profile. The space decreases when shoreline descends the slope to the maximum-regressive position, as indicated by the thick arrow beneath the shelf profile. The trend of change in subaerial accommodation space during transgression is opposite to that during regression. **B)** Postulated trend of total accommodation space (i.e., both submarine and subaerial) on the up-dip part of the Eastern Shelf over a cycle interval. The accommodation space is capped by a base level composed of two segments, the absolute sea level basinward of the shoreline and the graded river profile landward of the shoreline. No scale is intended.

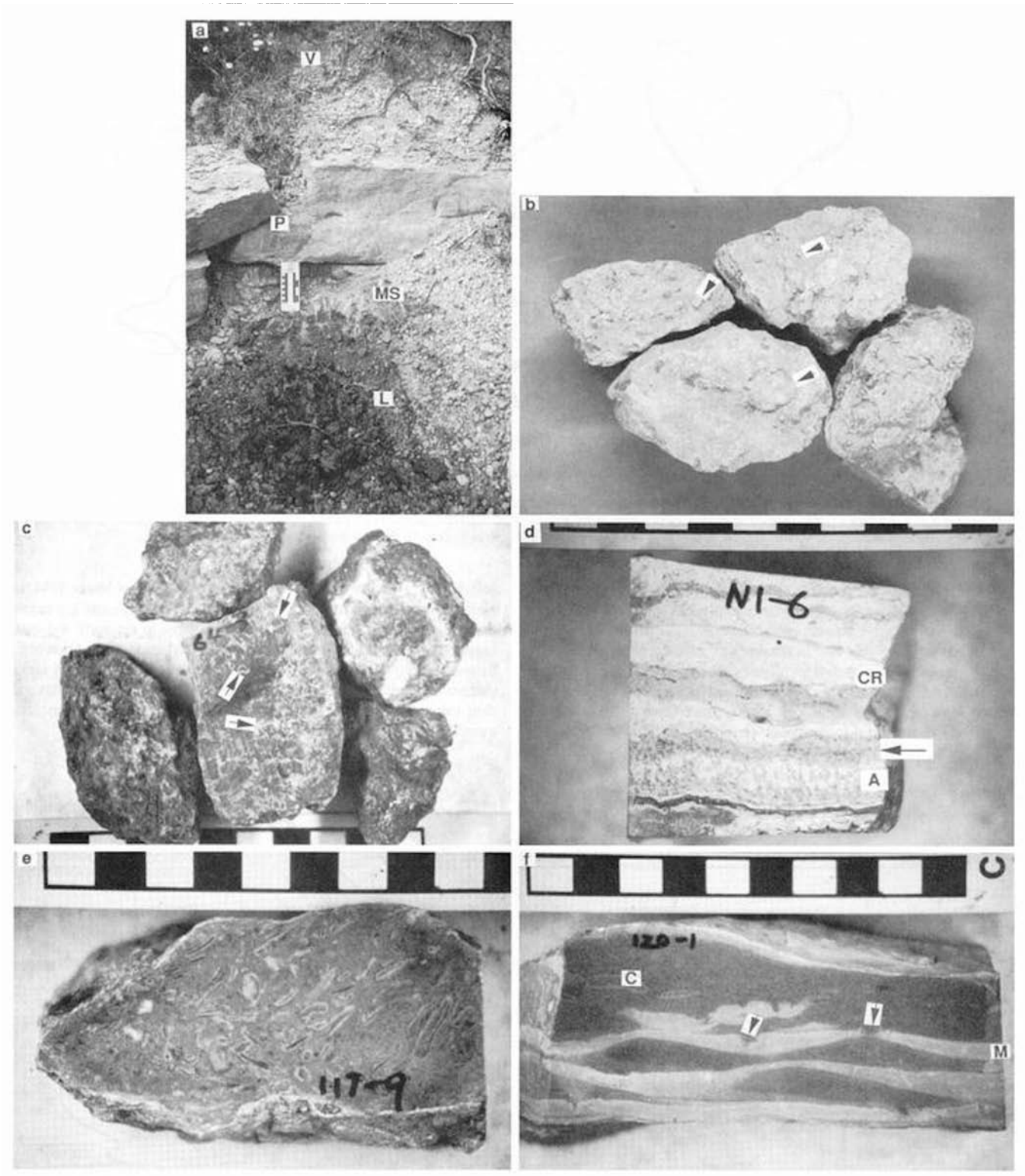

FIG. 15.—Some climate-sensitive lithofacies of the Cisco cycles. **A)** An early-transgression lignite (L) grades upward into a brown marginal-marine shale and a fossiliferous marly marine shale (MS) in the Waldrip Shale. The packstone (P) is well current-laminated in the lower part, and burrowed and shaly in the upper part; it grades upward into a red to maroon regressive vertisol (V). Scale is 10 cm. **B)** Flint clay nodules from beneath a calcareous and fossiliferous transgressive shale in the Wayland Shale. The nodules are dark gray to brownish gray, dense, non-slaking, nonfossiliferous, and full of oval to elongate nodules approximately 2 mm in diameter (arrows). The nodules are mainly composed of dickite (50%) and silica. **C)** Reddish-purple, dense, brecciated clay nodules from a variegated vertisol in the Salt Creek Bend Shale. Branching or radiating cracks resemble root networks and are filled with sparry or opaque pedogenic calcite (arrows). **D)** A reddish-cream caliche crust (CR) formed on a

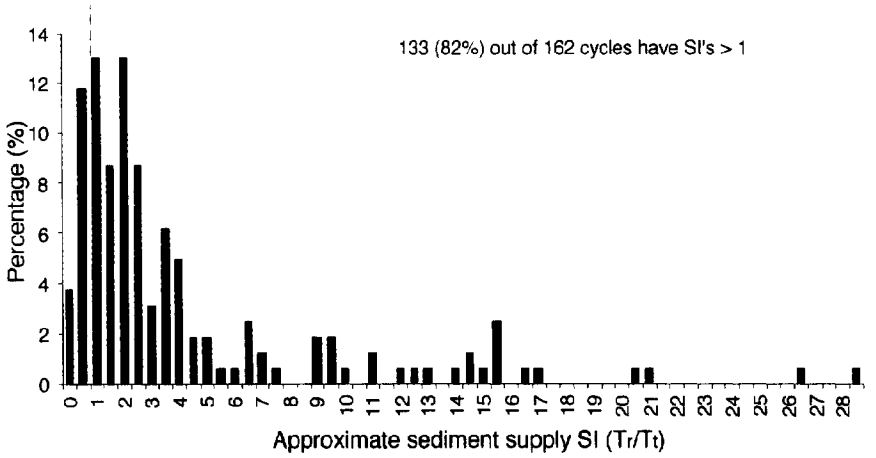

FIG. 16.—Distribution of the ratio of thickness of regressive deposits (T_r) to transgressive deposits (T_t). The ratio approximates the sediment-supply symmetry index. The dashed line indicates a symmetry-index value of one. Thicknesses of transgressive and regressive deposits of 162 Cisco cycles are used in the calculation.

Regressive clastic deposits are ferruginous and sandstone-rich, but rarely very carbonaceous, and contain abundant erosional surfaces, indicative of efficient sediment delivery and vigorous sedimentation during late regression (Fig. 9A, D). This pattern is more evident in the Brazos River valley close to major sediment sources to the north (Yang 1995). In general, nonmarine transgressive deposits are thin and poorly developed, and were mainly deposited in shoreline environments, whereas regressive deposits are thick and diverse, and were deposited in shoreline, delta-plain, and fluvial environments. A range of subenvironments are well developed during late regression, as indicated by frequent lateral facies changes. This is probably caused in part by the increase of subaerial accommodation space during late regression. Although both sediment supply and erosion increase during late regression, the former apparently dominated, enhancing preservation of Cisco sediments.

Evidence of autogenic control of cycle characteristics does not preclude allogenic processes being the dominant control on cycle symmetry. Many local variations of cycle characteristics can be filtered out by regional cycle correlation (e.g., Lee 1938; Brown 1960, 1962; Boardman and Malinky 1985; Yang 1995). Stratigraphic repetition of transgressive and regressive deposits is predictable throughout the Cisco Group because complex interactions of physical processes on a short time scale probably produce a predictable steady state on the cycle scale (Swift and Thorne 1991). The systematic variations of major allogenic processes, combined with an understanding of autogenic processes, are synthesized to develop a model of cyclic sedimentation for the outcrop Cisco Group, which may be useful in future studies of similar stratigraphic records.

STAGES OF CYCLE DEVELOPMENT

The interpreted interplay among glacio-eustasy, subsidence, climate, sediment yield and supply, and depositional dynamics during formation of the Cisco cycles is summarized in Figure 18.

Stage 1: Early Transgression (Fig. 18A).—Glacio-eustatic sea-level rise causes landward shoreline migration toward the depositional site—the up-dip part of the Eastern Shelf. Basement subsidence since the last regression, which increases away from the Bend Arch (Fig. 1), has steepened the shelf profile slightly, although subaerial erosion tends to compensate for this steepening. Continuous precipitation in a subhumid climate and rising groundwater table due to sea-level rise favor peat formation in back-barrier environments. High rainfall and runoff promote sediment yield in the upland. The subaerial accommodation space first increases, then decreases, storing some nonmarine sediments. Once the shoreline crosses the depositional site, sea water forms an effective littoral energy fence against sediment delivery, trapping most sediments in landward sinks on the coastal plains and in the drainage basins.

Fast transgression induced by rapid sea-level rise and augmented by a shallow shelf profile commonly prevents deposition of any nonmarine sediments and thick marine sediments. Shoreface erosion is limited by the low energy of the shallow, semi-restricted Eastern Shelf sea. Occasional pulses of terrestrial sediments may reach the site, some of which may persist into the late or maximum transgression, inhibiting and diluting carbonate deposition.

Stage 2: Late Transgression (Fig. 18B).—As the shoreline moves landward away from the site, normal marine conditions allow carbonate-secreting organisms to spread over the broad transgressive shelf. Initially, marine reworking promoted by limited sediment influx generates limestone conglomeratic lag and current-laminated coarse carbonate sediments. Deposition of supratidal carbonate and shoal-water nonskeletal grainstone is hindered by rapid deepening combined with the subhumid climate. As a result, transgressive limestones are thin and upward-deepening.

Stage 3: Maximum Transgression (Fig. 18C).—Submarine accommodation space is at its greatest extent as sea level rises to its maximum level while shelf subsidence and limited sedimentation continue. Hemipelagic and prodeltaic muds of core shales are slowly deposited, although upland sediment yield is at a maximum under a highly seasonal, wet-dry climate. Formation of phosphate nodules in some core shales suggests a dysoxic or anoxic environment below a thermocline, which is probably enforced by fresh/brackish water capping the water column (Heckel 1977; Soreghan 1994).

However, core shale is present in less than 50% of these cycles, and cycles with phosphate nodules are scarce, indicating that the depositional

←

regressive tidal-flat algal mat (A), and truncating algal heads (arrow), in the Gouldbusk Limestone. The crust is banded by alternating pure calcic and detritus-rich layers composed of dissolution breccias cemented in a calcic matrix. E) An *Osagia* packstone in the upper part of a regressive limestone in the Ivan Limestone. Micrite-coated and foram-encrusted grains are highly abraded and altered, ranging from 0.5 to 10 mm, mostly 2–6 mm in diameter. The matrix is lime mudstone and peloidal grainstone. F) A peloidal grainstone in the upper part of a regressive limestone in the Santa Anna Shale. It is graded and laminated, and locally is slightly burrowed. Lime mudstone layers (M) cap well-preserved ripple forms and contain desiccation cracks and borings (arrows). A few intraclasts (C) are present. It was probably deposited in an ephemeral, intertidal to supratidal pond. Locations are shown in Figure 1.

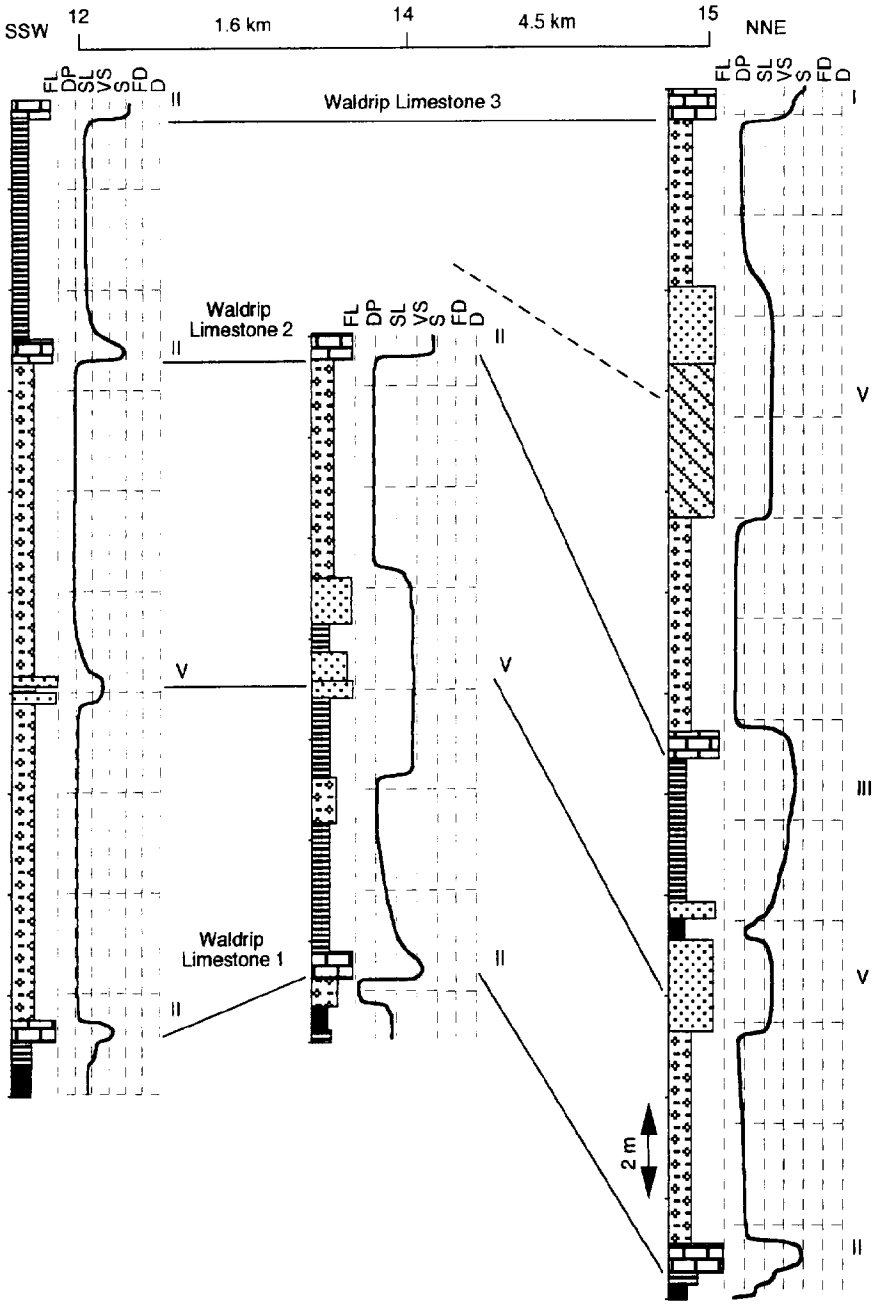

FIG. 17.—Lateral changes of cycle type, magnitude, and thickness as well as cycle disappearance in the Waldrip Shale in the Colorado River valley area. See Figure 5 for keys.

site was often not deep enough to deposit core shales. The magnitude of glacio-eustatic sea-level fluctuations varies over a wide range both in the Recent and in the late Paleozoic (Cronin 1983; Veevers and Powell 1987). It is assumed that core shale is deposited only when sea-level rise results in sufficient deepening. Often this is not the case, and coalesced transgressive and regressive limestones are deposited to form Type II cycles.

Stage 4: Early Regression (Fig. 18D).—The shoreline begins to move basinward. The submarine accommodation space remains large because: (1) transgressive accommodation space was mostly not filled by limited transgressive deposits; (2) sea-level drops slowly; and (3) siliciclastic sediments stored in landward sinks have not yet been delivered to the depositional site.

Sufficient accommodation and time facilitate active carbonate deposition. Shallowing-upward carbonates form at two stages—"catch-up" then "give-up". Approximately 35% of carbonate accumulation reaches sea level to deposit supratidal and shoal-water carbonates before being suppressed by turbidity due to siliciclastic influx. More commonly, carbonate deposition is quenched by siliciclastic sediments before reaching sea level, or in some cases, never occurs, as in cycle Types IV and V.

Stage 5: Late Regression (Fig. 18E).—Further sea-level drop slightly increases relief between the upland and the depositional site but greatly decreases the river gradient and enhances subaerial denudation before the shoreline migrates basinward to the shelf edge. The shoreline retreats closer to the depositional site, enabling river-mouth bypassing of sediments over

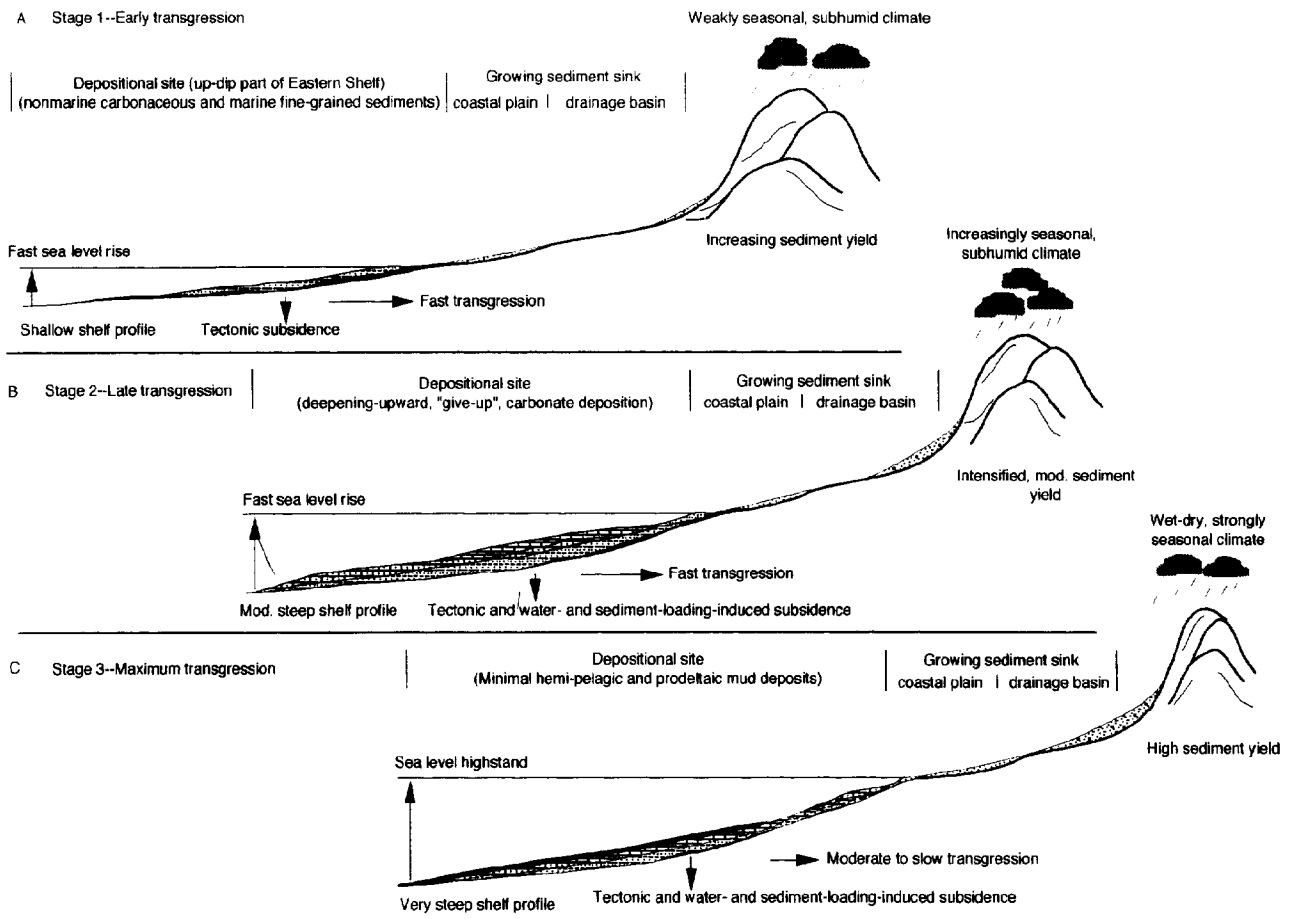

FIG. 18.—Schematic process–response model of cyclic sedimentation of the Cisco Group on the up-dip part of the Eastern Shelf during various stages of transgression and regression. The cross sections are oriented approximately west to east (Fig. 1). Although no scale is intended so as to show as many elements as possible, the relief is probably less than 100 m and the horizontal distance is less than 100 km at the depositional site. In contrast, the relief is probably around 1 km and the horizontal distance is few hundreds of kilometers in the areas of upland drainage basin and coastal plain. See Figure 5 for lithologic keys.

the littoral energy fence (Swift and Thorne 1991). The submarine accommodation space, partly filled by regressive limestones, is gradually filled by prograding and aggrading marine deltaic and associated marginal marine facies, followed by nonmarine delta-plain and fluvial facies.

The rate of submarine accommodation change is thought to be mainly controlled by the rate of eustatic sea-level change (Heckel 1984). The rates of Quaternary sea-level change are probably comparable to those of late Paleozoic sea-level change (Heckel 1986; Veevers and Powell 1987). Rates of sea-level falls are 0.2–1.6 cm/yr, whereas those of sea-level rises are 1–3 cm/yr (Cronin 1983). Thus, slow accommodation decrease due to slow sea-level drop may contribute considerably to the accumulation of thick marine and marginal-marine regressive deposits, and increased subsidence caused by sediment loading and compaction further enhances deposition and preservation.

Once the shoreline passes the depositional site, accommodation space is capped by the graded river profile. Decreasing river gradient may create a positive subaerial accommodation space, which allows delta-plain and fluvial facies to further aggrade. Much of the sediment supply may have come from landward sinks, where quantities of sediment were stored during transgression.

Stage 6: Maximum Regression (Fig. 18F).—Sea level drops below the shelf edge. Fluvial deposition on the now nearly flat shelf is minimal and erosion and sediment bypass through incised valleys dominate. Pedogenesis on the interfluves under a semiarid climate is intensive until a return to subhumid climate during the next transgression (Table 1).

SUMMARY

(1) Cycle symmetry compares the magnitude of environment shift and thickness between transgressive and regressive hemicycles. It is a measure of stratigraphic response. The asymmetry of the Cisco cycles indicates asymmetrical cyclic variations in controlling processes.

(2) Systematic variations of several allogenic processes control the asymmetry of Cisco cycles. Eustatic sea-level change and basement subsidence control accommodation; low-latitude glacial–interglacial climate, sediment yield in the source area, and sediment supply at the depositional site control sediment infilling of the accommodation space. The combined effects of these processes determine the magnitude and thickness/duration and, therefore, symmetry of transgressive–regressive cycles.

(3) Cycle symmetry is related to the rates of major processes controlling accommodation and sediment infilling. The relation can be used to understand and predict styles of transgressive and regressive sedimentation dictated by the relative dominance of processes controlling accommodation and those controlling sediment infilling during transgression and regression. Transgressive sedimentation was sediment-supply-controlled, whereas regressive sedimentation was accommodation-controlled on the Eastern

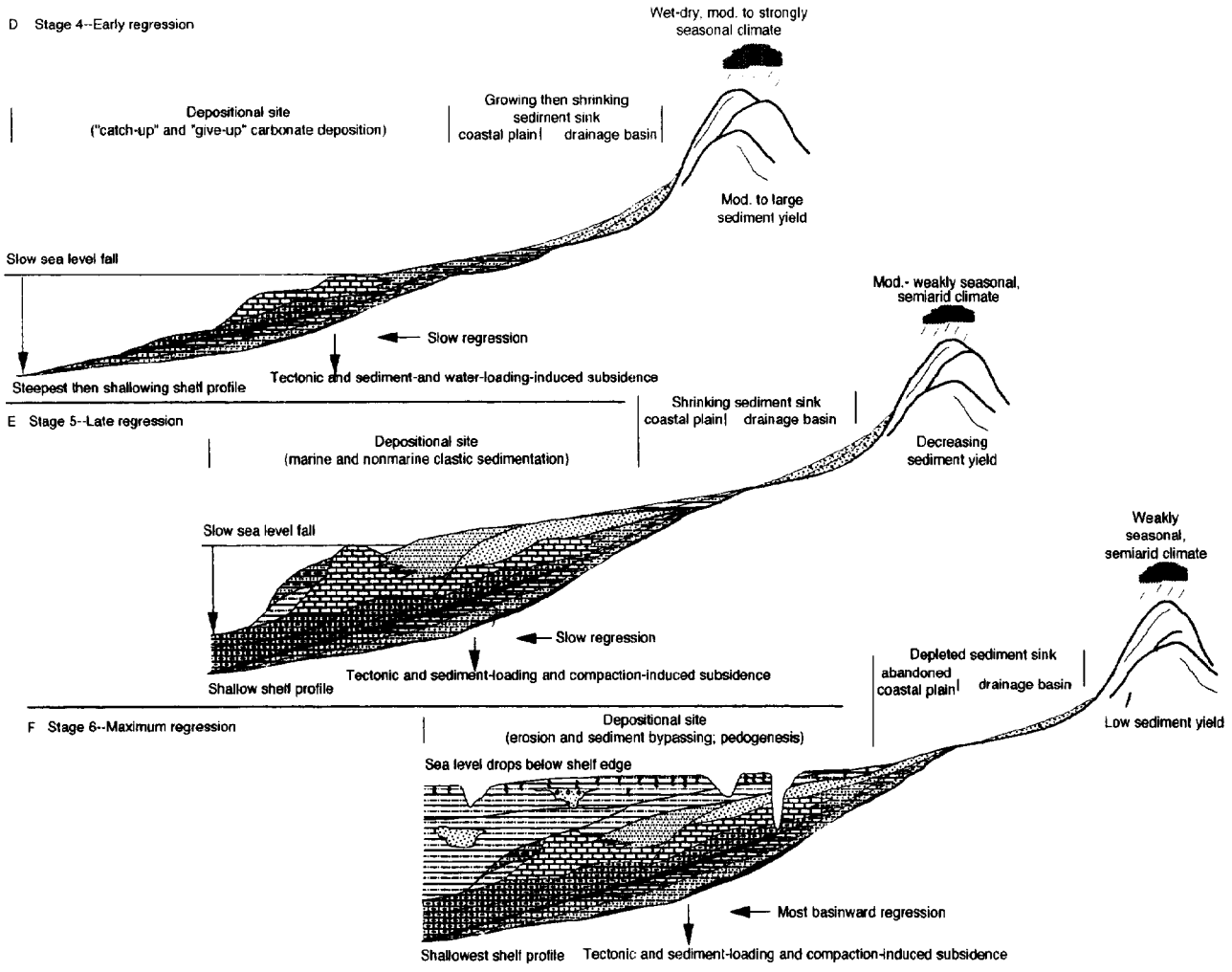

FIG. 18.—Continued.

Shelf. As a result, retrogradation and aggradation of transgressive deposits and aggradation and progradation of regressive deposits are expected.

(4) The sedimentary characters of Cisco cycles are controlled by both allogenic and autogenic processes. The latter include local topography, tectonics, and sedimentary processes governed by depositional dynamics. Five cycle types signify deviations from the systematic trends of allogenic processes controlling cycle symmetry.

(5) The proposed developmental stages of Cisco cycles integrate contemporaneous autogenic and allogenic processes. The interplay among these processes is invoked to explain the stratigraphic responses during various stages of transgression and regression. They provide a framework for understanding variable cycle characteristics at hemicycle and cycle scales.

ACKNOWLEDGMENTS

I extend my gratitude to Dr. M. Kominz for her consistent support and critical reviews at all stages of this study, and to W. Dharmasamadhi, M. Li, and C. Kellam for field assistance. Reviews by and stimulating discussions with C. Broquet and Dr. W. Galloway had great impacts on the content of this paper. Thoughtful reviews by Drs. R. Major and L.F. Brown, Jr., and by A. Molineaux, and JSR reviewers Drs. A. Eberli, A. Lomando, and J. Southard improved the manuscript significantly. This work was supported by the Geology Foundation of The University of Texas at Austin, the Gulf Coast Association of Geological Societies, and the Geological Society of America. Acknowledgment is made to the Donors of the Petroleum Research Fund, administrated by the American Chemical Society under grant ACS-PRF 20852-AC8 to M. Kominz, which provided partial support for this research.

REFERENCES

ALDIS, D.S., GROSSMAN, E.L., YANCEY, T.E., AND MCLERRAN, R.D., 1988, Isotope stratigraphy and paleodepth changes of Pennsylvanian sedimentary deposits: PALAIOS, v. 3, p. 487–506.

BARRELL, J., 1917, Rhythms and the measurements of geologic time: Geological Society of America, Bulletin, v. 28, p. 745–904.

BASSINOT, F.C., LABEYRIE, L.D., VINCENT, E., QUIDELLEUR, X., SHACKLETON, N.J., AND LANCELOT, Y., 1994, The astronomical theory of climate and the age of the Brunhes–Matuyama magnetic reversal: Earth and Planetary Science Letters, v. 126, p. 91–108.

BLUM, M.D., TOOMEY, R.S., III, AND VALASTRO, S., JR., 1994, Fluvial response to Late Quaternary climatic and environmental change, Edwards Plateau, Texas: Palaeogeography, Palaeoclimatology, Palaeoecology, v. 108, p. 1–21.

BOARDMAN, D.R., II, AND HECKEL, P.H., 1989, Glacial-eustatic sea-level curve for early Late Pennsylvanian sequence in north-central Texas and biostratigraphic correlation with curve for midcontinent North America: Geology, v. 17, p. 802–805.

BOARDMAN, D.R., II, AND MALINKY, J.M., 1985, Glacial-eustatic control of Virgilian cyclothems in north-central Texas, *in* McNulty, C.L., and McPherson, J.G., eds., American Association of Petroleum Geologists, Southwest Section, Transactions: Fort Worth Geological Society, p. 13–23.

BOND, G.C., AND KOMINZ, M.A., 1991, Some comments on the problem of using vertical facies changes to infer accommodation and eustatic sea-level histories with examples from Utah

and the southern Canadian Rockies, *in* Franseen, E.K., Watney, W.L., Kendall, C.G.St.C., and Ross, W., eds., Sedimentary Modeling: Computer Simulations and Methods for Improved Parameter Definition: Kansas Geological Survey, Bulletin 233, p. 273–291.

Brown, L.F., Jr., 1960, Stratigraphy of the Blach Ranch–Crystal Falls section (Upper Pennsylvanian), northern Stephens County, Texas: University of Texas at Austin, Bureau of Economic Geology, Report of Investigations no. 41, 45 p.

Brown, L.F., Jr., 1962, A stratigraphic datum, Cisco Group (Upper Pennsylvanian), Brazos and Trinity Valleys, north-central Texas: University of Texas at Austin, Bureau of Economic Geology, Report of Investigations no. 46, 42 p.

Brown, L.F., Jr., 1969, Virgil–lower Wolfcamp repetitive depositional environments in north-central Texas, *in* Elam, J.G., and Chuber, S., eds., Cyclic Sedimentation in the Permian Basin: West Texas Geological Society, p. 115–134.

Brown, L.F., Jr., Iriarte, R.F.S., and Johns, D.A., 1990, Regional depositional systems tracts, paleogeography, and sequence stratigraphy, Upper Pennsylvanian and Lower Permian strata, north-central Texas: The University of Texas at Austin, Bureau of Economic Geology, Report of Investigations no. 197, 116 p., 27 plates.

Bull, W.B., 1991, Geomorphic Responses to Climatic Change: New York, Oxford University Press, 326 p.

Cecil, C.B., 1990, Paleoclimate controls on stratigraphic repetition of chemical and siliciclastic rocks: Geology, v. 18, p. 533–536.

Chappell, J., and Shackleton, N.J., 1986, Oxygen isotopes and sea level: Nature, v. 324, p. 137–140.

Connolly, W.M., and Stanton, R.J., Jr., 1992, Interbasinal cyclostratigraphic correlation of Milankovitch band transgressive–regressive cycles: Correlation of Desmoinesian–Missourian strata between southeastern Arizona and the midcontinent of North America: Geology, v. 20, p. 999–1002.

Cronin, T.M., 1983, Rapid sea level and climate change: Evidence from continental and island margins: Quaternary Sciences Review, v. 1, p. 177–214.

Crowell, J.C., 1978, Gondwanan glaciation, cyclothems, continental positioning, and climate change: American Journal of Science, v. 278, p. 1345–1372.

Curray, J.R., 1964, Transgressions and regressions, *in* Miller, R.L., ed., Papers in Marine Geology: New York, Macmillan, p. 175–203.

Davies, D.J., and Hummell, R.L., 1994, Lithofacies evolution from transgressive to highstand systems tracts, Holocene of the Alabama coastal zone: Gulf Coast Association of Geological Societies, Transactions, v. 44, p. 145–153.

Galloway, W.E., and Brown, L.F., Jr., 1972, Depositional systems and shelf–slope relationships in Upper Pennsylvanian rocks, north-central Texas: The University of Texas at Austin, Bureau of Economic Geology, Report of Investigations no. 75, 62 p.

Goldhammer, R.K., Oswald, E.J., and Dunn, P.A., 1994, High-frequency, glacio-eustatic cyclicity in the Middle Pennsylvanian of the Paradox Basin: an evaluation of Milankovitch forcing, *in* de Boer, P.L., and Smith, D.G., eds., Orbital Forcing and Cyclic Sequences: International Association of Sedimentologists, Special Publication 19, p. 243–283.

Harrison, E.P., 1973, Depositional history of Cisco-Wolfcamp strata, Bend Arch, north-central Texas [unpublished Ph.D. thesis]: Texas Tech University, Lubbock, Texas, 189 p.

Heckel, P.H., 1977, Origin of phosphatic black shale facies in Pennsylvanian cyclothems of Midcontinent North America: American Association of Petroleum Geologists, Bulletin, v. 61, p. 1045–1068.

Heckel, P.H., 1984, Factors in mid-continent Pennsylvanian limestone deposition, *in* Hyne, N., ed., Limestones of the Midcontinent: Tulsa Geological Society, Special Publication 2, p. 25–50.

Heckel, P.H., 1986, Sea-level for Pennsylvanian eustatic marine transgressive–regressive depositional cycles along midcontinent outcrop belt, North America: Geology, v. 14, p. 330–334.

Imbrie, J., and Imbrie, J.Z., 1980, Modeling the climatic response to orbital variations: Science, v. 207, p. 943–953.

Klein, G. deV., and Willard, D.A., 1989, Origin of the Pennsylvanian coal-bearing cyclothems of North America: Geology, v. 19, p. 152–155.

Laporte, L.F., and Imbrie, J., 1964, Phases and Facies in the Interpretation of Cyclic Deposits: Kansas Geological Survey Bulletin 169, p. 249–263.

Leckie, D.A., 1994, Canterbury Plains, New Zealand—Implications for sequence stratigraphic models: American Association of Petroleum Geologists, Bulletin, v. 78, p. 1240–1256.

Lee, W., 1938, Stratigraphy of the Cisco Group of the Brazos Basin: University of Texas, Publication 3801, p. 11–90.

Mount, J.F., 1984, Mixing of siliciclastic and carbonate sediments in shallow shelf environments: Geology, v. 12, p. 432–435.

Muto, T., and Steel, R.J., 1992, Retreat of the front in a prograding delta: Geology, v. 20, p. 967–970.

Perlmutter, M.A., and Matthews, M.D., 1989, Global cyclostratigraphy—A model, *in* Cross, T.A., ed., Quantitative Dynamic Stratigraphy: New York, Prentice-Hall, p. 233–260.

Posamentier, H.W., Jervey, M.T., and Vail, P.R., 1988, Eustatic controls on clastic deposition I—Conceptual framework, *in* Wilgus, C.K., Hastings, B.S., Kendall, C.G.St.C., Posamentier, H.W., Ross, C.A., and Van Wagoner, J.C., eds., Sea-Level Changes—An Integrated Approach: SEPM, Special Publication 42, p. 109–124.

Roberts, H.H., Bailey, A., and Kuecher, G.J., 1994, Subsidence in the Mississippi River Delta—Important influences of valley filling by cyclic deposition, primary consolidation phenomena, and early diagenesis: Gulf Coast Association of Geological Societies, Transactions, v. 44, p. 619–629.

Ross, C.A., and Ross, J.R.P., 1985, Late Paleozoic depositional sequences are synchronous and worldwide: Geology, v. 13, p. 194–197.

Schumm, S.A., 1968, Speculations concerning paleohydrologic controls of terrestrial sedimentation: Geological Society of America, Bulletin, v. 79, p. 1573–1588.

Schutter, S.R., and Heckel, P.H., 1985, Missourian (early Late Pennsylvanian) climate in midcontinent North America: International Journal of Coal Geology, v. 5, p. 111–138.

Sloss, L.L., 1962, Stratigraphic models in exploration: American Association of Petroleum Geologists, Bulletin, v. 46, p. 1050–1057.

Soreghan, G.S., 1994, The impact of glacioclimatic change on Pennsylvanian cyclo-stratigraphy, *in* Embry, A.F., Beauchamp, B., and Glass, D.J., eds., Pangea: Global Environments and Resources: Canadian Society of Petroleum Geologists, Memoir 17, p. 523–543.

Swift, D.J.P., and Thorne, J.A., 1991, Sedimentation on continental margins, I: a general model for shelf sedimentation, *in* Swift, D.J.P., Oertel, G.F., Tillman, R.W., and Thorne, J.A., eds., Shelf Sand and Sandstone Bodies: Geometry, Facies and Sequence Stratigraphy: International Association of Sedimentologists, Special Publication 14, p. 3–31.

Tandon, S.K., and Gibling, M.R., 1994, Calcrete and coal in late Carboniferous cyclothems of Nova Scotia, Canada: Climate and sea level changes linked: Geology, v. 22, p. 755–758.

Tierrie, R.T., 1960, Geology of the Grosvenor Quadrangle, Texas, and petrology of some of its Pennsylvanian limestones [unpublished Ph.D. thesis]: The University of Texas at Austin, Austin, Texas, 172 p.

Veevers, J.J., and Powell, C.McA., 1987, Late Paleozoic glacial episodes in Gondwanaland reflected in transgressive–regressive depositional sequences in Euramerica: Geological Society of America Bulletin, v. 98, p. 475–487.

Wanless, H.R., and Shepard, F.P., 1936, Sea level and climatic changes related to late Paleozoic cycles: Geological Society of America, Bulletin, v. 38, p. 1177–1206.

Wermund, E.G., and Jenkins, W.A., Jr., 1969, Late Pennsylvanian Series in north-central Texas, *in* Wermund, E.G., and Brown, L.F., Jr., eds., A Guidebook to the Late Pennsylvanian Shelf Sediments, North-Central Texas: Dallas Geological Society, American Association of Petroleum Geologists–Society of Economic Paleontologists and Mineralogists, Annual Meeting, p. 1–11.

Wheeler, H.E., 1964, Baselevel, lithosphere surface, and time-stratigraphy: Geological Society of America, Bulletin, v. 75, p. 599–610.

Williams, D.F., 1988, Evidence for and against sea-level changes from the stable isotopic record of the Cenozoic, *in* Wilgus, C.K., Hastings, B.S., Kendall, C.G.St.C., Posamentier, H.W., Ross, C.A., and Van Wagoner, J.C., eds., Sea-Level Changes—An Integrated Approach: SEPM, Special Publication 42, p. 31–36.

Williams, D.F., Thunell, R.C., Tappa, E., Rio, D., and Raffi, I., 1988, Chronology of the Pleistocene oxygen isotope record 0–1.88 Million years B.P.: Palaeogeography, Palaeoclimatology, Palaeoecology, v. 64, p. 221–240.

Wilson, L., 1973, Variations in mean annual sediment yield as a function of mean annual precipitation: American Journal of Science, v. 273, p. 335–349.

Wilson, J.L., 1967, Cyclic and reciprocal sedimentation in Virgilian strata of Southern New Mexico: Geological Society of America, Bulletin, v. 78, p. 805–818.

Witzke, B.J., 1990, Palaeoclimatic constraints for Palaeozoic palaeolatitudes of Laurentia and Euramerica, *in* McKerrow, W.S., and Scotese, C.R., eds., Palaeozoic Palaeogeography and Biogeography: Geological Society of London, Memoir 12, p. 57–73.

Yancey, T.E., 1991, Controls on carbonate and siliciclastic sediment deposition on a mixed carbonate-siliciclastic shelf (Pennsylvanian Eastern Shelf of north Texas), *in* Franseen, E.K., Watney, W.L., Kendall, C.G.St.C., and Ross, W., eds., Sedimentary Modeling: Computer Simulations and Methods for Improved Parameter Definition: Kansas Geological Survey, Bulletin 233, p. 263–272.

Yang, W., 1995, Depositional cyclicity of the Cisco Group (Virgilian and Wolfcampian), North-central Texas [unpublished Ph.D. thesis]: The University of Texas, Austin, Texas, 268 p.

Received 1 March 1995; accepted 24 May 1996.